

An Exploration of the Scope of GPCR to RTK Transactivation
in HT22 and SH-SY5Y cells

by

Sean Newbury

A thesis

presented to the University of Waterloo

in fulfillment of the

thesis requirement for the degree of

Master of Science

in

Biology

Waterloo, Ontario, Canada, 2022

© Sean Newbury 2022

Author's Declaration

I hereby declare that I am the sole author of this thesis. This is a true copy of the thesis, including any required final revisions, as accepted by my examiners.

I understand that my thesis may be made electronically available to the public.

Abstract

Receptor tyrosine kinase (RTK) transactivation is a mechanism by which G protein-coupled receptor (GPCR) activity induces the activation of an RTK. As separate families of receptors, they were long thought to act independently. Transactivation demonstrates an interconnectedness between these families that complicates molecular signalling significantly. Currently, most research on transactivation focuses on specific GPCR-RTK pairs. This leaves broader questions about the nature of transactivation unanswered. It is not yet known whether transactivation is universal to all GPCRs and RTKs or limited only to certain receptors. Additionally, the physiological relevance of transactivation is also still unknown.

8 different GPCR agonists were used to transactivate PDGFR α to determine which GPCRs are capable of transactivation. To complement this, 3 GPCR agonists were used to transactivate a large number of RTKs simultaneously, to determine which RTKs are capable of being transactivated. These two experiments together provide a broad look at the receptors on both sides of transactivation. In addition, experiments were performed in both a mouse and human cell line, as well as both undifferentiated and differentiated cells. This provides information on whether transactivation acts similarly in different species, cell types, and stages of development. By beginning to answer these questions about the nature of transactivation, we can provide a better perspective on where future research can proceed.

Acknowledgements

First and foremost, I would like to thank my supervisor Dr. Mike Beazely. Your guidance and patience throughout my degree have been invaluable. I will always appreciate having the opportunity to work in your lab, and for taking me in when you did.

I would like to thank Dr. Dale Martin for being on my committee, and for offering the course I needed when none were available.

I would also like to thank Dr. Jonathan Blay for being on my committee, and for his words of encouragement when things weren't going so well.

I would also like to acknowledge the members of the Beazely Lab who helped me along the way. A special thank you to Morgan Robinson for all his help both in and out of the lab, and to James Livingstone and Kartar Singh for letting me use the last of the DMEM to finish my experiments. Quite literally couldn't have done it without you.

Finally, I thank my friends and family for all their support and encouragement.

Table of Contents

Author's Declaration.....	ii
Abstract.....	iii
Acknowledgements.....	iv
List of Figures.....	vi
List of Tables.....	viii
List of Abbreviations.....	ix
1.0 Introduction.....	1
1.1 G-Protein-Coupled Receptors.....	1
1.2 Receptor Tyrosine Kinases.....	4
1.3 RTK Transactivation.....	9
2.0 Objectives and Hypotheses.....	15
2.1 Exploration of GPCRs capable of transactivation.....	15
2.2 Exploration of RTKs capable of being transactivated.....	16
2.3 Determining if transactivation is consistent across species/cell types.....	16
3.0 Materials and Methods.....	17
3.1 Cell Culture Models used.....	17
3.2 Compound Preparations and Treatments.....	18
3.3 Western Blotting.....	20
3.4 Proteome Profiler Phospho-RTK Array Kits.....	22
3.5 Statistics.....	25
4.0 Results.....	26
4.1 Transactivation of PDGFR α	26
4.2 Transactivation by LP12, Quinpirole, and DAMGO.....	31
4.3 Transactivation in undifferentiated and differentiated HT22 cells.....	34
5.0 Discussion.....	37
5.1 Transactivation of PDGFR α	37
5.2 Transactivation by LP12, Quinpirole, and DAMGO.....	41
5.3 Transactivation in undifferentiated and differentiated HT22 cells.....	45
6.0 Conclusions and future directions.....	47
References.....	49
Appendix.....	56

List of Figures

Figure 1. Mechanism of GPCR activation	3
Figure 2. Mechanism of RTK activation	6
Figure 3. Mechanism of ERK1/2 activation	8
Figure 4. Mechanism of ligand-dependent transactivation	11
Figure 5. Mechanism of ligand-independent transactivation	13
Figure 6. Effect of various GPCR agonists on PDGFR α phosphorylation in HT22 cells	26
Figure 7. Effect of various GPCR agonists on ERK phosphorylation in HT22 cells	27
Figure 8. Effect of various GPCR agonists on PDGFR α phosphorylation in SH-SY5Y cells	28
Figure 9. Effect of various GPCR agonists on ERK phosphorylation in SH-SY5Y cells	29
Figure 10. Effect of quinpirole on various RTKs in HT22 cells	31
Figure 11. Effect of LP12, quinpirole, and DAMGO on insulin receptor in SH-SY5Y cells	32
Figure 12. Effect of LP12 on ErbB2, PDGFR α , Axl, EphA8, and IGF-IR in undifferentiated and differentiated HT22 cells	34
Figure 13. Effect of quinpirole on ErbB2, PDGFR α , Axl, EphA8, and IGF-IR in undifferentiated and differentiated HT22 cells	35
Figure 14. Time course of TrkB phosphorylation following LP12 treatment	55
Figure 15. Time course of TrkB phosphorylation following serotonin treatment	56
Figure 16. Time course of TrkB phosphorylation following quinpirole treatment	57

Figure 17. Time course of PDGFR α phosphorylation following LP12 treatment.....	57
Figure 18. Time course of PDGFR α phosphorylation following quinpirole treatment.....	58
Figure 19. Time course of ERK phosphorylation following LP12 treatment.....	59
Figure 20. Time course of ERK phosphorylation following quinpirole treatment.....	60
Figure 21. Imaged array membrane showing effects of PDGF-AA treatment	61

List of Tables

Table 1. Classification and characteristics of known GPCRs.....	2
Table 2. Classification and characteristics of human RTKs	5
Table 3. GPCR agonists used for transactivation.....	15
Table 4. Treatment concentrations and durations	18
Table 5. Protease and phosphatase inhibitors in Halt cocktail.....	20
Table 6. Antibodies used for western blotting	22
Table 7. RTK antibodies in mouse Proteome Profiler kit	24
Table 8. RTK antibodies in human Proteome Profiler kit.....	24
Table 9. Summary of results for transactivation of PDGFR α and activation of ERK	36

List of Abbreviations

ADAM: A disintegrin and metalloprotease

CHPG: Chlorohydroxyphenylglycine

DMSO: Dimethyl sulfoxide

D2R: D2 dopamine receptor

EGFR: Epidermal growth factor receptor

GPCR: G-protein-coupled receptor

HB-EGF: Heparin-binding EGF-like growth factor

HRP: Horseradish peroxidase

IGF-1R: Insulin-like growth factor receptor 1

INSR: Insulin receptor

LBD: Ligand-binding domain

MAPK: Mitogen-activated protein kinase

MMP: Matrix metalloproteinase

MOR: μ -opioid receptor

PBS: Phosphate-buffered saline

PTK: Protein tyrosine kinase

PTP: Protein tyrosine phosphatase

Ras-GAP: Ras GTPase activating protein

Ras-GEF: Ras guanine nucleotide exchange factor

ROS: Reactive oxygen species

RTK: Receptor tyrosine kinase

SEM: Standard error of the mean

SH2: Src Homology 2

1.0 Introduction

1.1 G-Protein-Coupled Receptors

G-protein coupled receptors (GPCRs) are the largest family of signalling proteins. With over 800 GPCR genes in humans, they are the primary mediators of a cell's response to extracellular signals. Some act as receptors to external signals, such as compounds we taste and smell, or photons of light ^[1]. Others act within the body, responding to signals from other cells such as hormones, neurotransmitters, and various other important molecules such as amino acids and fatty acids ^[1]. The variety of potential responses is enormous, with each signal molecule capable of activating several different GPCRs, and each GPCR able to have different downstream effects ^[1].

GPCR structure is well-conserved across families. All are composed of seven transmembrane α -helices, with an extracellular N-terminus and an intracellular C-terminus. The extracellular ligand-binding domain (LBD) varies in structure depending on the ligand and class of GPCR. The intracellular side is much more conserved, serving as a signal transduction region to allow the signal to be carried across the membrane ^[2].

The GPCR family is traditionally broken into 6 different classes, based primarily on LBD structure. Class A (rhodopsin-like) receptors form the largest group by far, with 80% of all GPCRs falling into this class ^[3]. Classes B and C make up most of the remaining receptors, while classes D, E, and F have far fewer members, and are often found in very few species. Because of this, classes D, E, and F are poorly studied compared to A, B, and C. Details about each classes' characteristics can be found in Table 1. Despite the differences in structure, GPCRs of all classes share a common mechanism of signal transduction. This is shown in Figure 1.

Table 1. Classification and characteristics of known GPCRs

Class		Characteristics of class
A	Rhodopsin-like receptors	LBD formed between α -helices ^[4]
B	Secretin receptor family	Use peptides as ligands, high-affinity portion of LBD at N-terminus ^[4]
C	Metabotropic glutamate-like	Receptors exist as dimers, Venus flytrap domain at N-terminus ^[4]
D	Fungal mating pheromone receptors	Unique to fungi, similar topology to Class A receptors ^[5]
E	Cyclic AMP receptors	Unique to certain species of slime mold ^[6]
F	Frizzled/Smoothed family receptors	Found in wide variety of eukaryotes, lack motifs crucial in other classes of GPCRs ^[7]

GPCR signalling pathways have enormous significance in drug development. Estimates show that ~35% of all clinically approved drugs target GPCRs either directly, or related proteins upstream or downstream of GPCRs ^{[8][9]}. With such a crucial role in pharmaceuticals, it is important to understand the downstream effects of GPCR activity, and therefore of drugs that target GPCRs. By doing this, we can investigate potential side effects and interactions with other pathways, improving patient care and opening new possibilities for future drug development.

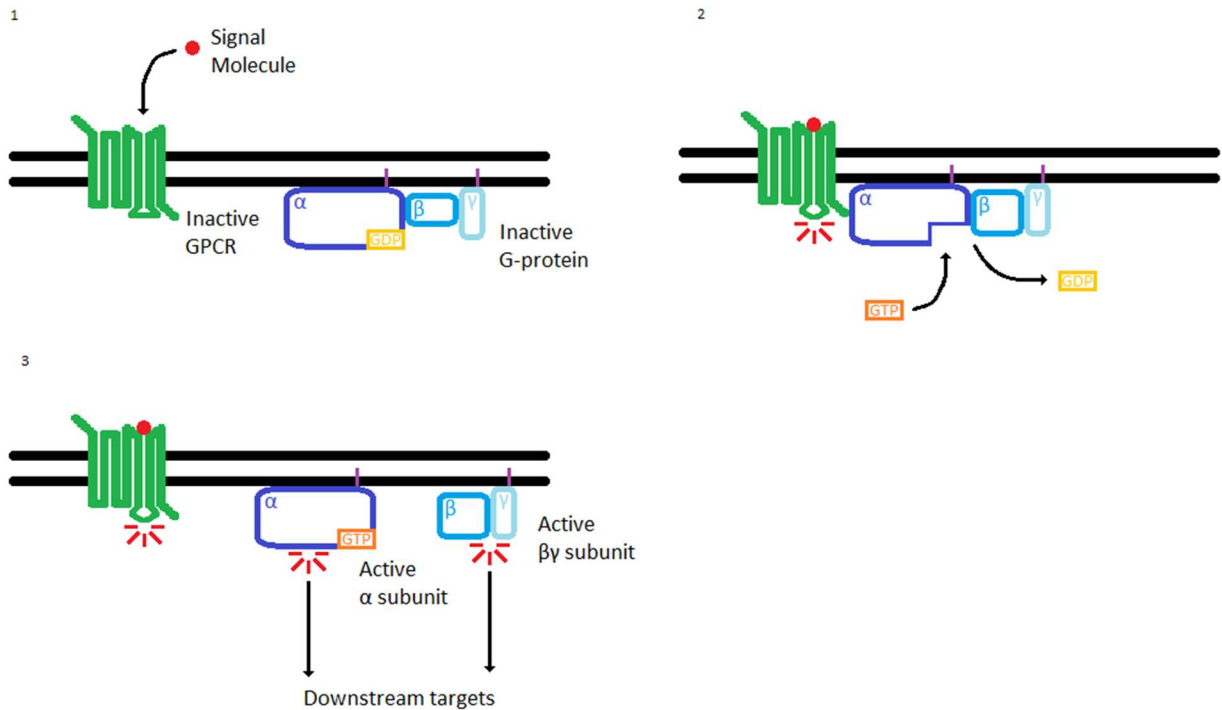


Figure 1. Mechanism of GPCR activation. The GPCR and associated G-protein begin in an inactive state. In this state, the GPCR is unable to bind the G-protein, and the G-protein forms a heterotrimeric complex composed of its α , β , and γ subunits, with a GDP molecule bound to the α -subunit. The α -subunit and γ -subunit are tethered to the intracellular membrane through covalent-attached lipid molecules. When ligand binds the GPCR, the relative positions of the α -helices shift, causing a conformational change on the intracellular side. This change allows the GPCR to bind the associated G-protein. The G-protein then exchanges its GDP molecule for a GTP molecule, and the $\beta\gamma$ complex dissociates from the α -subunit. The α -subunit and $\beta\gamma$ complex are then able to independently regulate their respective downstream targets [1][4].

1.2 Receptor Tyrosine Kinases

Receptor Tyrosine Kinases (RTKs) are not as numerous as GPCRs, but act as regulators of key cellular processes. This typically includes cell growth, proliferation, differentiation, survival, and migration ^[10]. Because of their important roles, mutations in RTK genes and their pathways are implicated in many diseases, especially cancers ^{[11][12]}. Overexpression, genomic amplification, and chromosomal rearrangements involving RTK genes have all been linked to different forms of cancer ^[13].

Broadly speaking, RTKs consist of an extracellular receptor domain and an intracellular tyrosine kinase domain connected by a single transmembrane α -helix ^[10]. There are 58 RTK genes in humans, divided into 20 subfamilies depending on the structure of their extracellular domain. These are described in detail in Table 2 ^[11].

Most RTKs share the same mechanism of signal transduction. Ligand-binding induces dimerization of the RTKs, allowing each RTK to phosphorylate the tyrosine residues of the other ^[10]. This process is described in detail in Figure 2. There are exceptions to this mechanism, however. For example, in epidermal growth factor receptors (EGFRs), rather than crosslinking two separate receptors, the ligand instead binds to a single receptor at two sites, inducing a conformational change that allows it to bind to another ligand-bound receptor ^[11]. The dimer formed is asymmetric, with only one receptor's tyrosine kinase domain becoming active, phosphorylating tyrosine residues for both receptors ^[1].

Table 2. Classification and characteristics of human RTKs ^[11].

Class	Family Name	Members	Molecular characteristics of the extracellular domains
I	EGFR	EGFR, ERBB2, ERBB3, ERBB4	2 cysteine-rich domains
II	Insulin R	INSR, IGFR	2 chains α and β , with one cysteine-rich and 2 FNIII domains
III	PDGFR	PDGFR α , PDGFR β , M-CSFR, KIT, FLT3L	5 Ig-like domains
IV	VEGFR	VEGFR1, VEGFR2, VEGFR3	7 Ig-like domains
V	FGFR	FGFR1, FGFR2, FGFR3, FGFR4	3 Ig-like domains, 1 acidic box
VI	CCK	CCK4	7 Ig-like domains
VII	NGFR	TRKA, TRKB, TRKC	2 Ig-like domains, rich leucin domains
VIII	HGFR	MET, RON	1 transmembrane α chain linked with one extracellular β chain
IX	EPHR	EPHA1-EPHA6, EPHB1-EPHB6	1 Ig-like, 1 cysteine-rich, and 2 FNIII-like domains
X	AXL	AXL, MER, TYRO3	2 Ig-like, 2 FNIII-like domains
XI	TIE	TIE, TEK	2 Ig-like, 1 EGF, 3 FNIII-like domains
XII	RYK	RYK	1 transmembrane β chain linked with one extracellular α chain.
XIII	DDR	DDR1, DDR2	1 discoidin-like domain
XIV	RET	RET	1 cadherin-like domain
XV	ROS	ROS	6 FNIII-like domains
XVI	LTK	LTK, ALK	1 cysteine-rich domains
XVII	ROR	ROR1, ROR2	1 Ig-like domain, 1 cysteine-rich domain, and 1 kringle-like domain
XVIII	MUSK	MUSK	4 Ig-like and 1 cysteine-rich domains
XIX	LMR	AATYK1, AATYK2, AATYK3	A short extracellular domain
XX	Undetermined	RTK106	A short receptor chain with a short extracellular domain

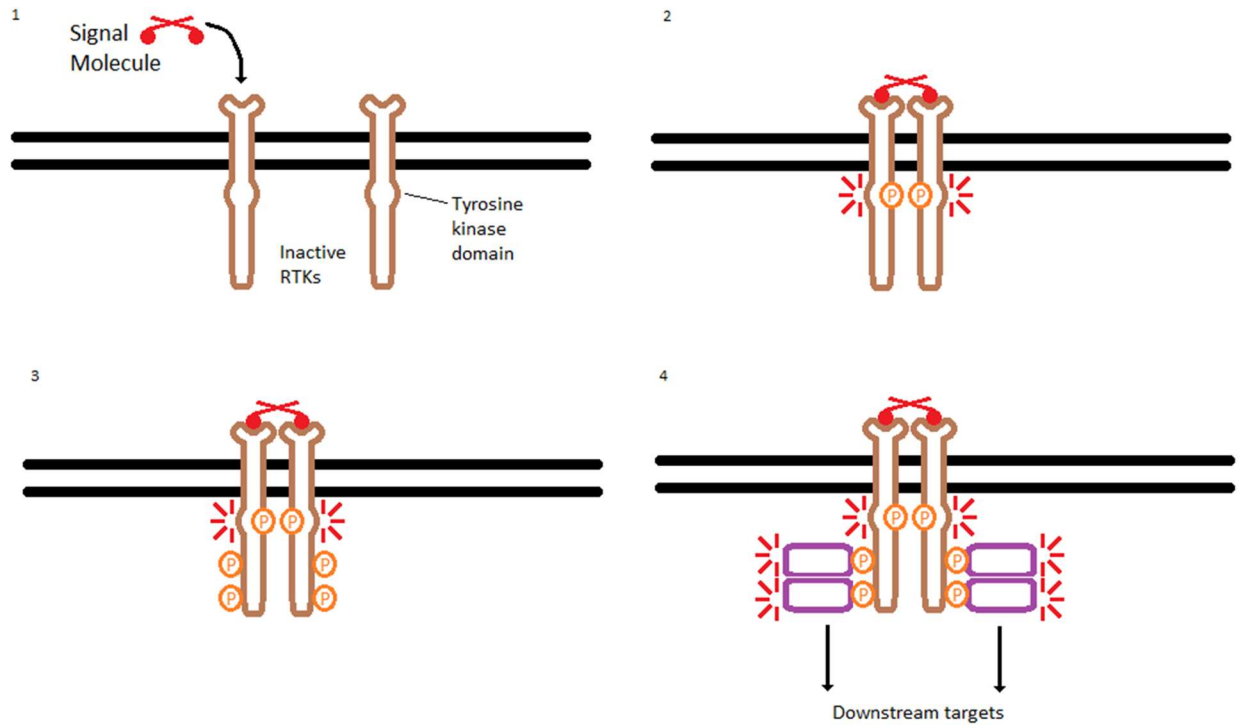


Figure 2. Mechanism of RTK activation. The RTKs begin as two separate inactive monomers. The bivalent ligand simultaneously binds two RTK proteins, drawing them together to form a dimer. In this form, intracellular tyrosine kinase domains phosphorylate tyrosine residues on the opposite RTK, forming docking sites. Many signalling proteins contain Src Homology 2 (SH2) domains or phosphotyrosine-binding domains. These domains recognize and bind to phosphotyrosine on the RTK, becoming active in doing so ^{[1][10]}.

One of the most important effects of RTKs is the activation of extracellular signal-regulated kinases (ERKs). ERKs form one of three subgroup of the mitogen-activated protein kinase (MAPK) family alongside c-Jun N-terminal kinases and p38 MAPKs ^[14]. Specifically, ERK1 and ERK2 serve a crucial role in RTK signalling by converting the short-lived signals of RTKs into more sustained ones to alter gene expression and protein activity in what is called the MAPK/ERK pathway. The result of this is the increased cell growth, differentiation, and division typical of RTK activation ^[1]. Like RTKs, mutations in MAPK/ERK pathway proteins can result in increased proliferation and inhibition of apoptosis, leading to tumorigenesis ^{[1][15]}.

The MAPK/ERK pathway is downstream of Ras proteins, a family of monomeric GTPases ^[1]. Signalling proteins associated with an activated RTK in turn activate Ras, either through the activation of a Ras guanine nucleotide exchange factor (Ras-GEF) or through the inhibition of a Ras GTPase-activating protein (Ras-GAP). Ras-GEFs stimulate dissociation of the bound GDP molecule, allowing a GTP molecule to take its place, activating Ras. Ras-GAPs instead increase the rate of GTP hydrolysis by Ras, deactivating it. Inhibition of Ras-GAPs therefore promotes Ras activation ^[1]. Ras activity in turn initiates the kinase cascade that makes up the MAPK/ERK pathway, composed of the MAPKK kinase Raf, the MAPK kinase MEK, and finally the MAP kinases ERK1/2. This results in activation of transcription factors, affecting gene expression, as well as various other proteins ^{[1][15]}. This process is shown below in Figure 3.

Since the MAPK pathway is downstream of most RTKs, it is a useful measure of RTK transactivation. Being associated with several RTKs as opposed to only one allows us to measure the net effect of several RTKs being transactivated simultaneously.

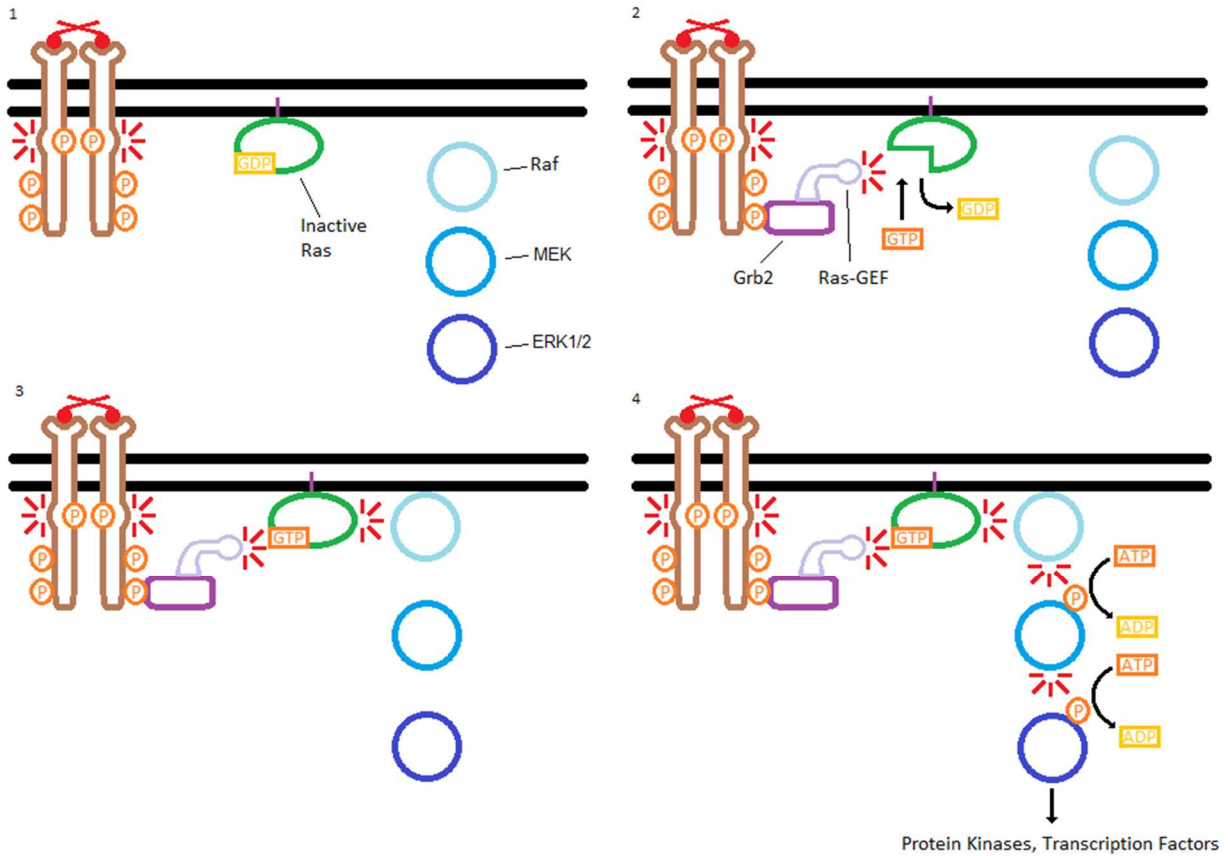


Figure 3. Mechanism of ERK1/2 activation. The Ras protein begins in an inactive state. Upon activation of the RTK, docking sites are formed by the phospho-tyrosine residues. Grb2 contains SH2 domains that recognize and bind to these sites. Grb2 also contains SH3 domains that bind to Ras-GEF, which stimulates the inactive Ras protein to replace its bound GDP with GTP, causing it to become active. In this activated state, Ras recruits Raf to the plasma membrane and activates it. Raf then phosphorylates MEK, which then phosphorylates ERK1/2. ERK1/2 are then able to phosphorylate their downstream targets [1][15].

Like GPCRs, RTKs are also important receptors in drug development. Due to their involvement in cancers, there are many anti-cancer drugs that act as RTK inhibitors by attenuating RTK activity and inducing apoptosis in cancer cells ^{[11][12][13]}. These include monoclonal antibodies that target RTKs and small molecule kinase inhibitors ^{[16][17][18]}. Unfortunately, cancer cells often develop resistance to these inhibitors after repeated use, making them ineffective over long periods of time ^{[12][18]}. They can also often have significant toxic side effects on the patient ^[17]. Because of these problems, development of new ways to inhibit RTK activity is an important area of pharmaceutical research.

1.3 RTK Transactivation

Broadly speaking, RTK Transactivation is a pathway in which GPCR activity causes the activation of an RTK as a downstream target. The term “transactivation” was first used in 1996 to describe a way by which EGFR could be activated in the absence of its ligand ^[19]. Though much transactivation still focuses on EGFR, this phenomenon has been found in many other RTKs as well. This pathway is interesting, as it goes against what one would typically expect from receptor signalling. As receptors, RTKs are typically activated by very specific signals. Under transactivation, they are instead activated as a downstream target of GPCR signalling ^[20]. This creates an enormous number of possibilities depending on expression patterns of GPCRs and RTKs in a given cell. Though the focus of this thesis is RTK transactivation, it is worth mentioning that GPCR transactivation is also possible, whereby RTK activity can induce activation of a GPCR ^[21]. This highlights the interconnectedness of these signalling pathways previously thought to function independently. Due to this complexity, it is important to

understand the scope of these processes. Determining which GPCRs and RTKs are capable of this activity is an integral step in understanding the mechanism of RTK transactivation.

RTK transactivation can occur in either a ligand-dependent pathway or a ligand-independent pathway. The ligand-dependent pathway relies on the shedding of membrane-bound RTK pro-ligand by matrix metalloproteinases (MMPs) or ADAMs (short for “a disintegrin and metalloproteinase”). This mechanism is also called “Triple-Membrane-Passing-Signal”, as the signal crosses the membrane three times: with the GPCR, the MMP, and finally the RTK ^[20]. This process is shown in greater detail in Figure 4 below.

The MMPs/ADAMs involved depend on cell type and original GPCR stimulus. In cardiomyocytes, angiotensin II receptor type 1 activates ADAM17, causing shedding of heparin-binding EGF-like growth factor (HB-EGF), which then activates EGFR ^[20]. In ACHN cells, ADAM10 is instead responsible. MMP-2, MMP-7, MMP-9, and ADAM12 have also been found to be involved in shedding of HB-EGF in various cell types ^[20].

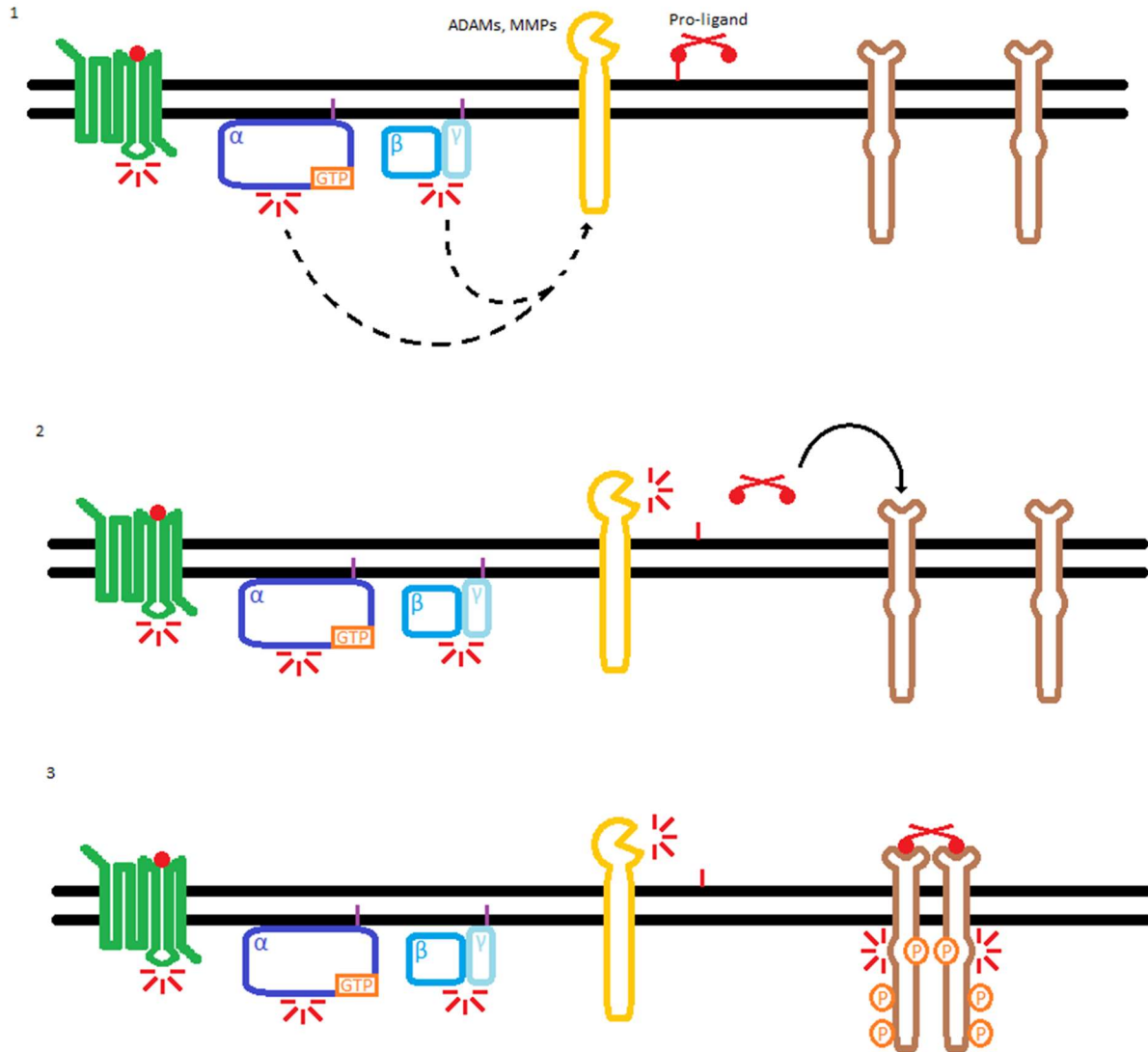


Figure 4. Mechanism of ligand-dependent transactivation. The RTK ligand begins as extracellularly bound pro-ligand. One of the downstream targets of GPCR activity is the activation of MMPs. MMP activation can occur through many different intermediate targets including PKC and Src [20][22][23]. These MMPs cleave the pro-ligand from the membrane, allowing it to bind to and activate its associated RTK. Under this mechanism, the RTK is activated by ligand produced by the cell the RTK is bound to, as opposed to an external signal [20].

Ligand-independent transactivation, as its name suggests, activates the RTK without use of its ligand. Instead of the typical autophosphorylation seen in RTKs, the tyrosine residues are instead phosphorylated by protein tyrosine kinases (PTKs) downstream of GPCRs. In this way, docking sites can be formed without activation of the receptor, and without requiring dimerization. This mechanism is dependent on reactive oxygen species (ROS) produced by nicotinamide adenine dinucleotide phosphate (NADPH) oxidase [20]. These ROS inhibit the activity of protein tyrosine phosphatases (PTPs), preventing them from immediately dephosphorylating the RTK. This process is described in more detail in Figure 5 below. Recent research suggests that the GPCR and RTK must be physically associated in a receptor heterocomplex for ligand-independent transactivation to occur [24].

Many of these heterocomplexes have been identified. For example, TrkB has been found to complex with D1 and D2 dopamine receptors (D1R and D2R), type 2 angiotensin receptors, and type 1 cannabinoid receptors [24]. This transactivation seems to provide a neuroprotective effect, and even antidepressant effects in some cases [24]. In addition, serotonin is capable of transactivating TrkB, and can increase its expression when exposed for longer periods [24][25]. Taken together, this would suggest a strong possibility that TrkB transactivation could have a significant role in the effects of selective serotonin reuptake inhibitors and other antidepressants. Other known complexes involved in transactivation include EGFR complexing with adenosine A1 receptor and D2R, and PDGFR β complexing with D2L and D4 dopamine receptors [24].

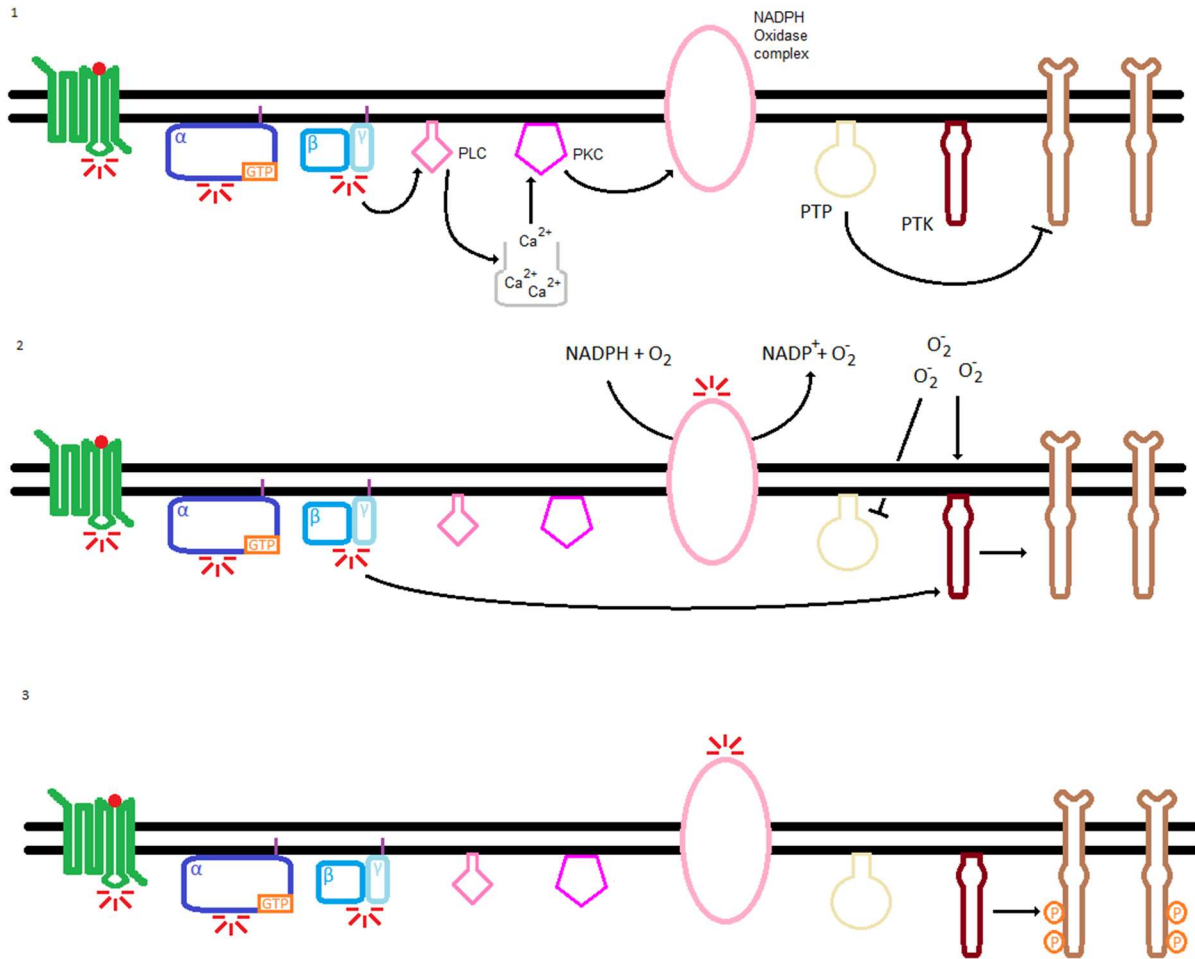


Figure 5. Mechanism of ligand-independent transactivation. One target of G-proteins are PTKs. These can phosphorylate the tyrosine residues present on RTKs, but PTP activity suppresses this, preventing the RTK from being reliably activated. G-proteins can also activate the NADPH oxidase complex through a pathway involving PLC-induced Ca²⁺ release activating PKC and finally the NADPH oxidase complex. NADPH oxidase converts NADPH and O₂ into NADP⁺ and O₂⁻, a ROS. These ROS both inhibit PTP activity and enhance PTK activity. This shifts the equilibrium of intracellular tyrosine phosphorylation activity in favour of the PTKs, which are then able to successfully phosphorylate the RTKs' tyrosine residues, creating docking sites necessary for downstream signalling [20][25].

Given the importance of GPCRs and RTKs as drug targets, it is worthwhile to consider RTK transactivation within the context of pharmacology. Through transactivation, drugs that target GPCRs could have effects on RTK signalling, leading to unintended side effects or unanticipated interactions with RTK-targeting drugs. There may be benefits as well, however, as recent research has shown that transactivation can have neuroprotective effects on cells [26].

Cancer is one area of research where intentionally targeting transactivation for the purposes of treatment could be beneficial. Many GPCRs are overexpressed in different cancer types, contributing to tumorigenesis and metastasis. Protease-activated receptors (PARs) are one group of GPCRs currently being researched for its role in certain cancers [27][28]. Though relatively few in number, there are GPCR-targeting drugs approved for use against different cancers [29]. This, combined with RTKs being well-established targets of anti-cancer drugs makes transactivation an intriguing possibility for cancer research. A pathway that connects two groups of receptors both involved in cancer could provide new targets for drug development.

Most research on RTK transactivation involves specific GPCR-RTK pairs in cell lines overexpressing the target(s) of interest, and often overstimulates the GPCR far beyond what would be seen in a physiological system. While this research is important in understanding the specific mechanisms behind each pathway, it often fails to address broader questions about the nature of transactivation in general, and its *in vivo* physiological purpose and relevance. This thesis seeks to begin answering some of these questions by exploring whether transactivation is a universal process of GPCRs and RTKs, or if it is limited to particular GPCRs and RTKs, and whether it is consistent between different species and cell types.

2.0 Objectives and Hypotheses

2.1 Exploration of GPCRs capable of transactivation

One aim of the thesis was to determine which GPCRs are capable of transactivation. 8 GPCR agonists were chosen and assessed via western blot for their effect on PDGFR α and ERK activation. These can be seen below in Table 3.

Table 3. GPCR agonists used for transactivation.

GPCR agonist	Target Receptor	Receptor Family	Class
LP12	5-HT7R	Serotonin	A
LP44	5-HT7R	Serotonin	A
8-OH-DPAT	5-HT1AR	Serotonin	A
Quinpirole	D2R	Dopamine	A
CHPG	mGluR5	Metabotropic Glutamate	C
AMN082	mGluR7	Metabotropic Glutamate	C
DAMGO	MOR	Opioid	A
Baclofen	GABA β R	GABA	C

These were chosen to represent a variety of GPCRs across several families and two classes. Furthermore, multiple GPCRs within serotonin and metabotropic glutamate receptors were targeted to allow comparison within those families and determine if transactivation remains consistent within a family.

It was hypothesized that the GPCR agonists used would transactivate PDGFR α and activate ERK. Results in literature have shown all GPCR targets used except mGluR7 exhibit transactivation behaviour, albeit with different cell types and with different RTK targets in most cases ^{[30][31][32][33][34][35]}. It was further hypothesized that families of GPCRs would exhibit similar levels of PDGFR α transactivation.

2.2 Exploration of RTKs capable of being transactivated

The second aim of the thesis was to determine which RTKs are capable of being transactivated. Cells were treated with LP12, quinpirole, and DAMGO and assessed using the Proteome Profiler Phospho-RTK Array kit (R&D systems ARY014 and ARY001B) to determine transactivation effects on 39 or 49 RTKs for the mouse and human versions, respectively.

It was hypothesized that transactivation would be seen in some, but not all RTKs. Literature review and previous experiments performed targeting PDGFR α showed that LP12, quinpirole, and DAMGO were capable of transactivation for multiple RTKs, and so it was presumed they could transactivate other RTKs as well. However, since not all RTKs will be expressed in a single cell line, it was not expected that all RTKs would show results.

2.3 Determining if transactivation is consistent across species/cell types

The third aim of this thesis was to compare transactivation results between different cell lines to determine if transactivation remains consistent across different species and cell types. Experiments addressing aims 2.1 and 2.2 were performed in both a mouse cell line (HT22) and human cell line (SH-SY5Y), allowing comparison between the two cell lines. Additionally, transactivation results in undifferentiated and differentiated HT22 cells were compared to determine if the process of differentiation changes transactivation.

It was hypothesized that transactivation would be different between different cell types. Different cell types express different receptors, which should change how transactivation acts between them.

3.0 Materials and Methods

3.1 Cell Culture Models used

The model systems used were HT22 cells and SH-SY5Y cells. HT22 cells are mouse hippocampal neuron-derived cells. They are often used as a hippocampal neuronal model due to their origin. There are significant differences between the undifferentiated and differentiated form, as they gain cholinergic properties and become susceptible to excitotoxicity upon differentiation ^[36]. This large shift in signalling properties made them suitable for comparing transactivation before and after differentiation. SH-SY5Y cells are a human neuroblastoma-derived cell line taken from a metastatic bone tumor. They are commonly used in research on neuronal function and differentiation, as well as neurodevelopmental disorders ^[37]. As a human cancer cell line, results in this model could have relevance to the previously discussed possibility of transactivation as a target for cancer treatment.

HT-22 cells were grown in 10 cm² culture dishes. Media used was composed of DMEM/F12 and 10% fetal bovine serum. Cells were kept at 37°C and 5% CO₂. Cells were grown until they reached 70% confluency, then differentiated with neurobasal media containing N2 supplement and 2mM L-glutamine for 24 hours. Drug treatments were performed in neurobasal media.

SH-SY5Y cells were grown in 10 cm² culture dishes. Media used was composed of DMEM/F12 and 15% fetal bovine serum. Cells were kept at 37°C and 5% CO₂. Cells were grown until they reached 80% confluency, then differentiated with neurobasal media containing N2 supplement and 2 mM L-glutamine for 24 hours. Drug treatments were performed in neurobasal media.

3.2 Compound Preparations and Treatments

Eight different GPCR agonist compounds were used as treatments in these experiments. The treatments are described in Table 4, and the details of their preparation are described below. Treatment durations were chosen based on what has been used in literature, as well as time courses performed observing effects of LP12, serotonin, and quinpirole on TrkB, PDGFR α , and ERK. These time courses can be seen in the Appendix, Figures 14-16, 17-18, and 19-20 respectively.

Table 4. Treatment concentrations and durations

Treatment	Treatment concentration	Treatment duration
LP12	300 nM	10 or 20 minutes
LP44	300 nM	10 minutes
8-OH-DPAT	10 nM	5 minutes
Quinpirole	10 μ M	10 minutes
CHPG	2 mM	10 minutes
AMN082	10 μ M	10 minutes
DAMGO	100 nM	5 minutes
Baclofen	100 μ M	1 or 5 minutes

LP12 stock solutions were prepared by dissolving in dimethyl sulfoxide (DMSO) to 5 mM concentration and stored at -20°C. On the day of treatment, a small amount of the stock was further diluted to 300 μ M with MilliQ water. From this, 1 μ L was added to the cells to bring the final concentration to 300 nM. The final concentration of DMSO was 0.006%. Treatment duration was 20 minutes unless otherwise stated.

LP44 stock solutions were prepared by dissolving in DMSO to 10 mM concentration and stored at -20°C. On the day of treatment, a small amount of the stock was further diluted to 300 μ M with a solution of 1:2 DMSO:phosphate-buffered saline (PBS). From this, 1 μ L was added to

the cells to bring the final concentration to 300 nM. The final concentration of DMSO was 0.035%. Treatment duration was 10 minutes.

8-OH-DPAT stock solutions were prepared by dissolving in DMSO to 10 mM concentration and stored at -20°C. On the day of treatment, a small amount of the stock was further diluted to 10 µM with a solution of 1:5 DMSO:PBS. From this, 1 µL was added to the cells to bring the final concentration to 10 nM. The final concentration of DMSO was 0.017%. Treatment duration was 5 minutes.

Quinpirole stock solutions were prepared by dissolving in DMSO to 10 mM concentration and stored at -20°C in 10 µL aliquots. On the day of treatment, an aliquot was defrosted, and 1 µL was added to the cells to bring the final concentration to 10 µM. The final concentration of DMSO was 0.1%. Treatment duration was 10 minutes unless otherwise stated.

Chlorohydroxyphenylglycine (CHPG) solutions were prepared on the day of treatment by dissolving in 50 mM NaOH to a concentration of 50mM. From this, 40 µL was added to the cells to bring the final concentration to 2 mM. Treatment duration was 10 minutes.

AMN082 stock solutions were prepared by dissolving in DMSO to 10 mM concentration and stored at -20°C. On the day of treatment, a small amount of the stock was further diluted to 1 mM with MilliQ water. From this, 10 µL was added to the cells to bring the final concentration to 10 µM. The final concentration of DMSO was 0.1%. Treatment duration was 10 minutes

DAMGO stock solutions were prepared by dissolving in DMSO to 10 mM concentration and stored at -20°C. On the day of treatment, a small amount of the stock was further diluted to 100 µM with PBS. From this, 1 µL was added to the cells to bring the final concentration to 100 nM. The final concentration of DMSO was 0.001%. Treatment duration was 5 minutes.

Baclofen solutions were prepared on the day of treatment by dissolving in MilliQ water to a concentration of 10 mM. From this, 10 μ L was added to the cells to bring the final concentration to 100 μ M. Treatment duration was either 1 minute or 5 minutes.

A note about controls and DMSO: In all cases, vehicle controls using MilliQ water were used. While that is not the true vehicle in all cases, concentrations of PBS and DMSO were low enough that there should be no significant impact on results. Additionally, experiments comparing MilliQ water vehicle control to DMSO-treated cells at the highest concentration used (0.1%) were performed, with no significant difference between them.

3.3 Western Blotting

Western blotting was primarily used to determine the effect of the GPCR agonists previously described on PDGFR α and ERK. PDGFR α was chosen due to an experiment showing its expression and activation by PDGF-AA. This can be seen in the Appendix, Figure 21.

Western blotting was also used in the time courses seen in the Appendix, Figures 14-20.

After treatment, cells were rinsed in ice-cold PBS, and lysed by shearing with 26-gauge syringes in Lysis Buffer 17 (R&D systems 895943), with 1% Halt protease and phosphatase inhibitor cocktail (Thermo Fisher 78440) added. Inhibitors present in the Halt cocktail are presented in Table 5. Lysates were then centrifuged at 15,000 x g for 30 minutes at 4°C to remove debris. Supernatant was taken, and either frozen for later use or used immediately.

Table 5. Protease and phosphatase inhibitors in Halt cocktail.

Inhibitor	Target
Sodium Fluoride	Ser/Thr and Acidic Phosphatases
Sodium Orthovanadate	Tyr and Alkaline Phosphatases
β -glycerophosphate	Ser/Thr Phosphatases
Sodium Pyrophosphate	Ser/Thr Phosphatases
Aprotinin	Ser Proteases
Bestatin	Amino-peptidases
E64	Cysteine Proteases
Leupeptin	Ser/Cys Proteases

A bicinchoninic acid (BCA) protein assay was used to quantify protein concentration in lysates immediately prior to using them.

Lysates were mixed with 3x loading buffer (240 mM Tris-HCl at pH 6.8, 6% w/v SDS, 30% v/v glycerol, 0.02% w/v bromophenol blue, 50 mM DTT, and 5% v/v β -mercaptoethanol) and boiled at 95°C for 5 minutes. Samples were loaded at 15 μ g of protein per well and separated by SDS-PAGE. Gels were composed of an 8% resolving gel and a 4% stacking gel. Running buffer was composed of 25mM Tris base at pH 8.3, 0.1% w/v SDS, and 190mM glycine. Proteins were then transferred to a nitrocellulose membrane (wet transfer, 90 minutes at 100V). Transfer buffer was composed of 25 mM Tris base, 190 mM glycine, and 20% v/v methanol.

Membranes were stained with Ponceau and imaged using the Invitrogen iBright 1500F imaging station. Membranes were cut in half to allow different antibodies to be used on upper and lower halves. Ponceau stain was removed, and membranes were blocked for 1 hour at room temperature with blocking buffer composed of 5% non-fat milk in TBS-T (20 mM Tris base, 150mM NaCl, 0.1% Tween, pH 7.6). Membranes were then incubated in primary antibody in blocking buffer for 1 hour at room temperature, or overnight (16 hours) at 4°C. Membranes were then washed in TBS-T three times, followed by incubation in secondary antibody conjugated to

horseradish peroxidase (HRP) in blocking buffer for 1 hour at room temperature. Membranes were again washed in TBS-T three times, followed by short incubation in Western chemiluminescent substrate (Luminata Crescendo – Millipore). Membranes were again imaged in the Invitrogen iBright 1500F imaging station. After imaging, membranes were stripped and re-probed with β -actin antibody, if needed. Images were analyzed in iBright Analysis Software to determine local background corrected volumes for each sample, which were then normalized to control. Details on the antibodies used are described below in Table 6.

Table 6. Antibodies used for western blotting.

Antibody	Concentration	Incubation	Secondary used
PDGFR α , pTyr849	1:250	16 hours	Anti-rabbit
PDGFR α	1:500	16 hours	Anti-rabbit
TrkB, pTyr816	1:500	1 hour	Anti-rabbit
TrkB	1:1000	1 hour	Anti-rabbit
pERK	1:1000	1 hour	Anti-rabbit
ERK	1:1000	1 hour	Anti-rabbit
pGSK	1:1000	1 hour	Anti-rabbit
GSK	1:1000	1 hour	Anti-rabbit
β -actin	1:500	1 hour	Anti-mouse
Anti-rabbit secondary	1:5000	1 hour	N/A
Anti-mouse secondary	1:10,000	1 hour	N/A

3.4 Proteome Profiler Phospho-RTK Array Kits

The Proteome Profiler kit was used to determine the effects of LP12, quinpirole, and DAMGO on many RTKs simultaneously, to determine which RTKs are capable of being transactivated.

After treatment, cells were rinsed in ice-cold PBS, and lysed by shearing with 26-gauge syringes in Lysis Buffer 17 (R&D systems 895943), with 1% Halt protease and phosphatase inhibitor cocktail (Thermo Fisher 78440) added. Inhibitors present in the Halt cocktail are

presented in Table 5. Lysates were then centrifuged at 15,000 x g for 30 minutes at 4°C to remove debris. Supernatant was taken, and either frozen for later use or used immediately.

A BCA protein assay was used to quantify protein concentration in lysates immediately prior to using them.

Lysates were diluted to a concentration of 1.4 µg/µL (350 µg in 250 µL), then mixed with 1.25 mL of array buffer 1 (R&D Systems 895477). Arrays were blocked for 1 hour using array buffer 1. Arrays were then incubated in the prepared cell lysates overnight for 16 hours at 4°C. Arrays were then washed in wash buffer (R&D Systems 895003) three times for 10 minutes each time. Anti-Phospho-Tyrosine-HRP detection antibody (R&D Systems 841403) was diluted 1:5000 in array buffer 2 (R&D Systems 895477). Arrays were incubated in detection antibody for 2 hours at room temperature. Arrays were again washed in wash buffer three times, followed by a short incubation in Western chemiluminescent substrate (Luminata Crescendo – Millipore). Arrays were imaged in the Invitrogen iBright 1500F imaging station. Images were analyzed in iBright Analysis Software to determine local background corrected volumes for each sample, which were then normalized to control. Dots were not detected automatically and had to be manually identified within the software.

RTK antibodies present on the mouse and human versions of the kit can be found below in Tables 7 and 8, respectively. An example of the membrane can be seen in the Appendix, Figure 21.

Table 7. RTK antibodies in mouse Proteome Profiler kit. RTKs are arranged in the positions they appear on the membrane of the kit.

EGF R	HGF R	TrkC	EphB2
ErbB2	MSP R	VEGF R1	EphB4
ErbB3	PDGF R alpha	VEGF R2	EphB6
ErbB4	PDGF R beta	VEGF R3	
FGF R2 (IIIc)	SCF R	MuSK	
FGF R3	Flt-3	EphA1	
FGF R4	M-CSF R	EphA2	
Insulin R	c-Ret	EphA3	
IGF-I R	Tie-1	EphA6	
Axl	Tie-2	EphA7	
Dtk	TrkA	EphA8	
Mer	TrkB	EphB1	

Table 8. RTK antibodies in human Proteome Profiler kit. RTKs are arranged in the positions they appear on the membrane of the kit.

EGF R	Mer	Tie-2	EphA6
ErbB2	HGF R/c-Met	TrkA	EphA7
ErbB3	MSP R/Ron	TrkB	EphB1
ErbB4	PDGF R alpha	TrkC	EphB2
FGF R1	PDGF R beta	VEGF R1/Flt-1	EphB4
FGF R2 alpha	SCF R/c-kit	VEGG R/KDR	EphB6
FGF R3	Flt-3/Flk-2	VEGF R/Flt-4	ALK/CD246
FGF R4	M-CSF R	MuSK	DDR1
Insulin R/CD220	c-Ret	EphA1	DDR2
IGF-I R	ROR1	EphA2	EphA5
Axl	ROR2	EphA3	EphA10
Dtk	Tie-1	EphA4	EphB3
			Ryk

3.5 Statistics

In all cases, data was presented as relative change in phosphorylation compared to control. All error bars shown represent standard error of the mean (SEM).

A one-way ANOVA with a Dunnett's post-hoc test was used to analyze results for western blots of PDGFR α and ERK in both HT22 and SH-SY5Y cells, as well as Proteome Profiler kit results in SH-SY5Y cells, as these had several treatments being compared to a single control.

An unpaired t-test was used to analyze results for the Proteome Profiler kit results in HT22 cells, as this had a single treatment being compared to a single control, for multiple target RTKs being measured.

4.0 Results

4.1 Transactivation of PDGFR α

Both HT22 cells and SH-SY5Y cells were treated with 8 different GPCR agonists. Phosphorylation of PDGFR α and ERK were assessed by western blot to determine if transactivation was occurring in PDGFR α and/or in other RTKs as well. PDGFR α was chosen due to previous experiments showing it is expressed and functional in HT22 cells. This can be seen in the Appendix, Figure 21. Figures 6 and 7 below show the results for HT22 cells. Figure 6 shows PDGFR α phosphorylation, while Figure 7 shows ERK phosphorylation. From these figures, it can be seen that PDGFR α transactivation appears to occur to varying degrees for all treatments used, while ERK's signal seems to reduce.

An identical experiment was performed in SH-SY5Y cells, as seen in Figures 8 and 9. Results show a decrease in PDGFR α phosphorylation following treatment for most compounds used, with baclofen being an exception. ERK was activated by some compounds, while others reduced its signal or left it unchanged.

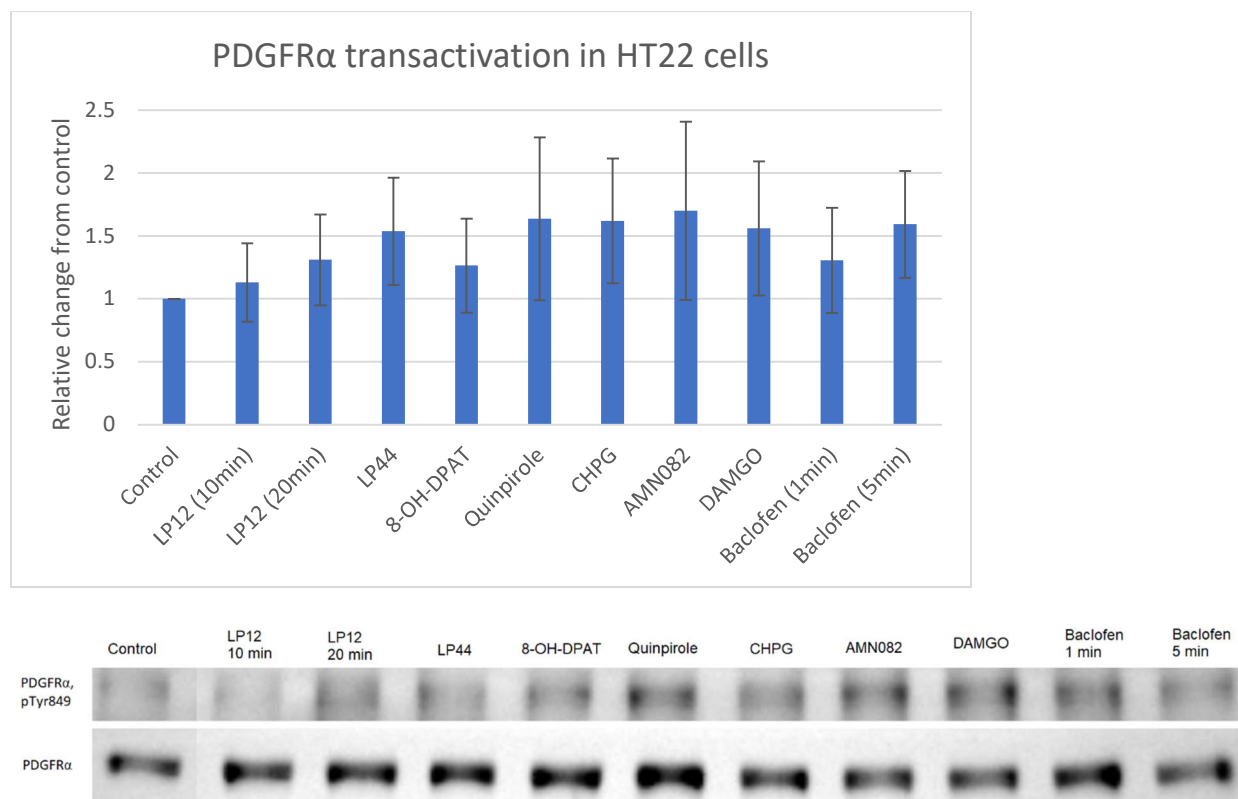


Figure 6. Effect of various GPCR agonists on PDGFR α phosphorylation in HT22 cells.

pPDGFR α data were normalized to total PDGFR α expression and expressed as relative change compared to control. Results are shown as mean \pm SEM. Statistical analysis was done using a one-way ANOVA with Dunnett's post-hoc test ($\alpha=0.05$, $n=4$). Western blot images have been spliced to better align bands.

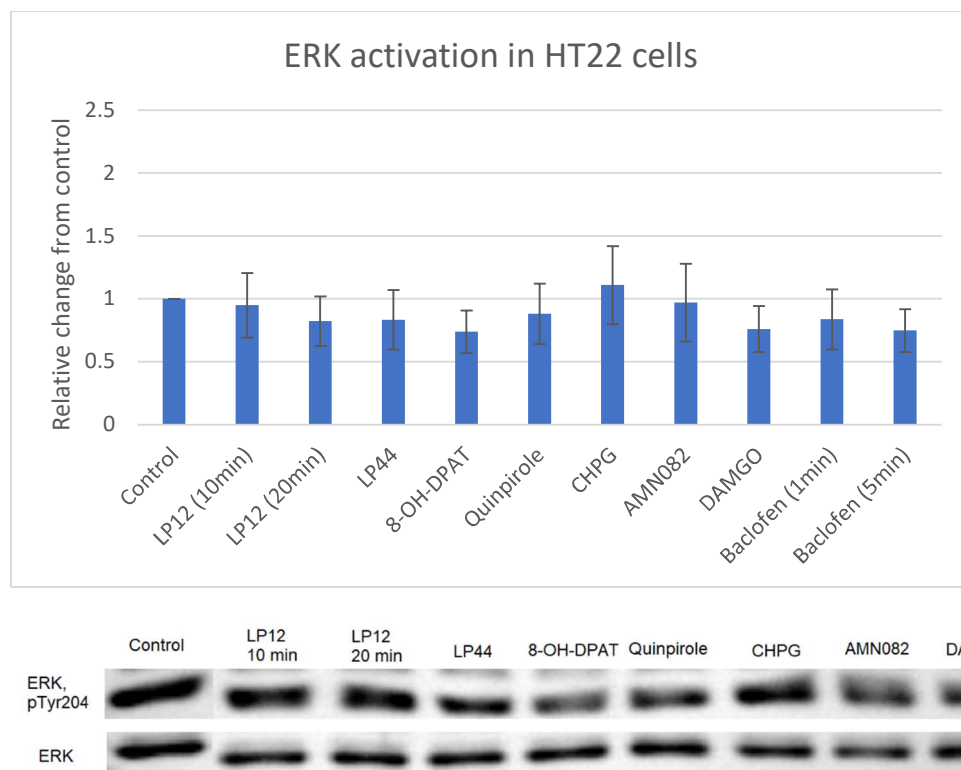


Figure 7. Effect of various GPCR agonists on ERK phosphorylation in HT22 cells. pERK data were normalized to total ERK expression and expressed as relative change compared to control. Results are shown as mean \pm SEM. Statistical analysis was done using a one-way ANOVA with Dunnett's post-hoc test ($\alpha=0.05$, $n=3$). Western blot images have been spliced to better align bands.

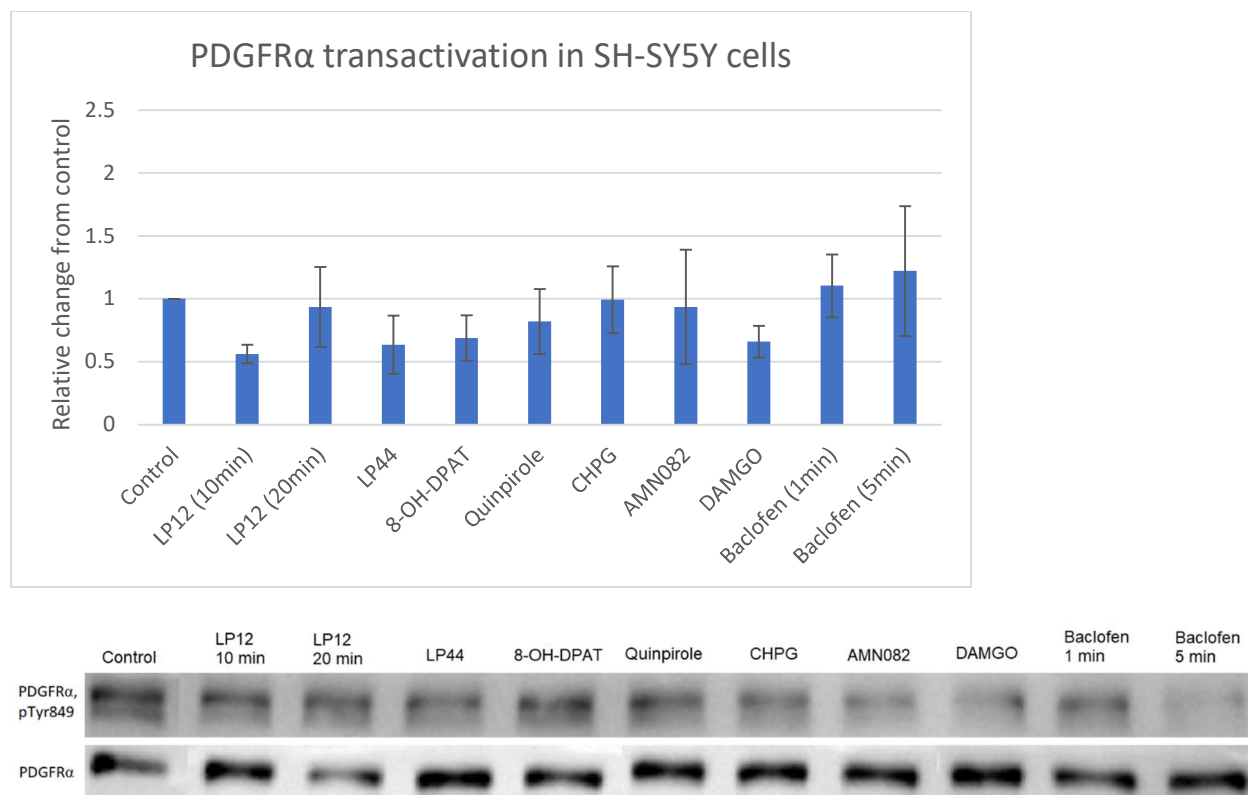


Figure 8. Effect of various GPCR agonists on PDGFR α phosphorylation in SH-SY5Y cells. pPDGFR α data were normalized to total PDGFR α expression and expressed as relative change compared to control. Results are shown as mean \pm SEM. Statistical analysis was done using a one-way ANOVA with Dunnett's post-hoc test ($\alpha=0.05$, $n=4$). Western blot images have been spliced to better align bands.

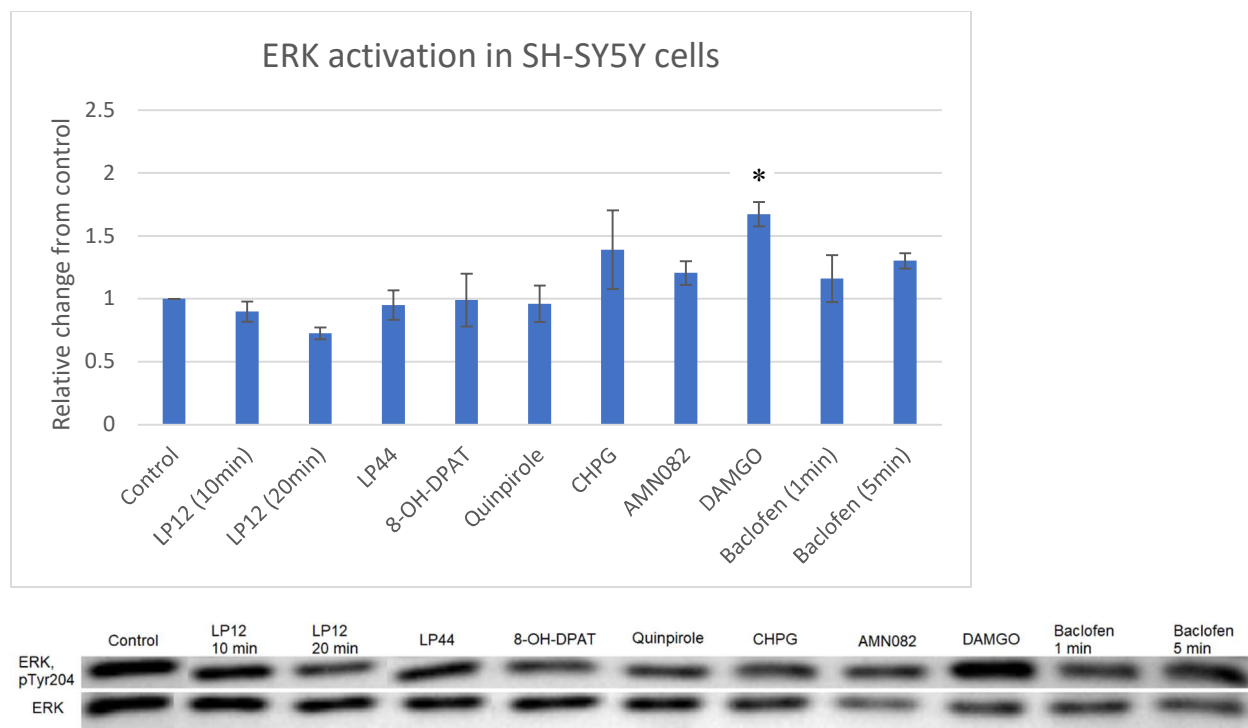


Figure 9. Effect of various GPCR agonists on ERK phosphorylation in SH-SY5Y cells. pERK data were normalized to total ERK expression and expressed as relative change compared to control. Results are shown as mean \pm SEM. Statistical analysis was done using a one-way ANOVA with Dunnett's post-hoc test ($\alpha=0.05$, $n=4$). A significant difference was observed between DAMGO-treated cells and control ($p<0.05$) Western blot images have been spliced to better align bands.

4.2 Transactivation by LP12, Quinpirole, and DAMGO

HT22 cells were treated with quinpirole to determine which RTKs, if any, showed evidence of transactivation following treatment. Lysates were analyzed using the Proteome Profiler Phospho-RTK Array Kit. Four RTKs produced signals strong enough to be detected. These were ErbB2, PDGFR α , Axl, and IGF-IR. Quinpirole treatment resulted in very little change to all RTKs observed.

A similar experiment was performed in SH-SY5Y cells, with LP12, quinpirole, and DAMGO. Though the kit contains antibodies to 39 and 49 RTKs for the mouse and human kits, respectively, unfortunately only very few were expressed at levels high enough to be detected by the kit. Only insulin receptor (INSR) produced a strong enough signal to be detected by the kit. All three treatments used caused a reduction in INSR phosphorylation. The results for these experiments can be seen in Figures 10 and 11.

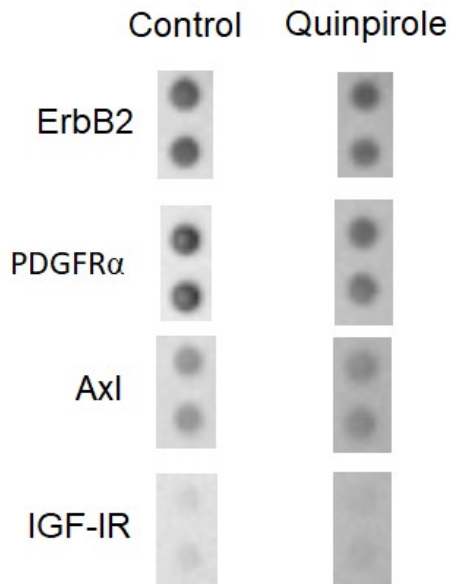
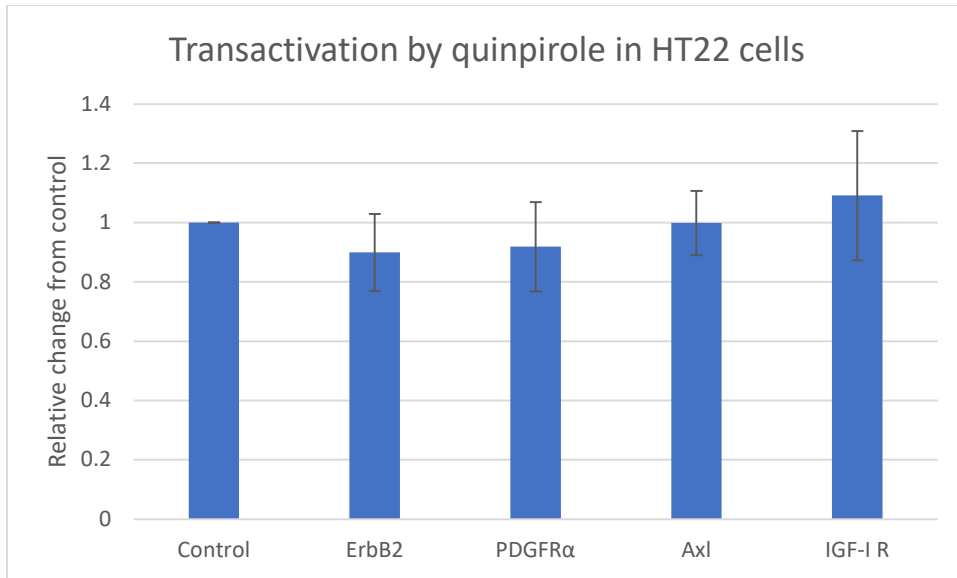


Figure 10. Effect of quinpirole on various RTKs in HT22 cells. RTK phosphorylation data was expressed as relative change compared to control. Results are shown as mean \pm SEM. Statistical analysis was done using an unpaired t-test with each RTK from the treated group being compared to its respective control (n=3). Array images have been spliced to show appropriate dots for each RTK.

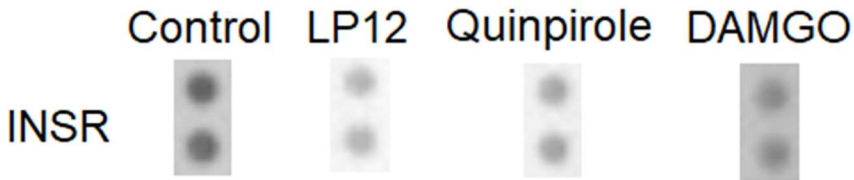
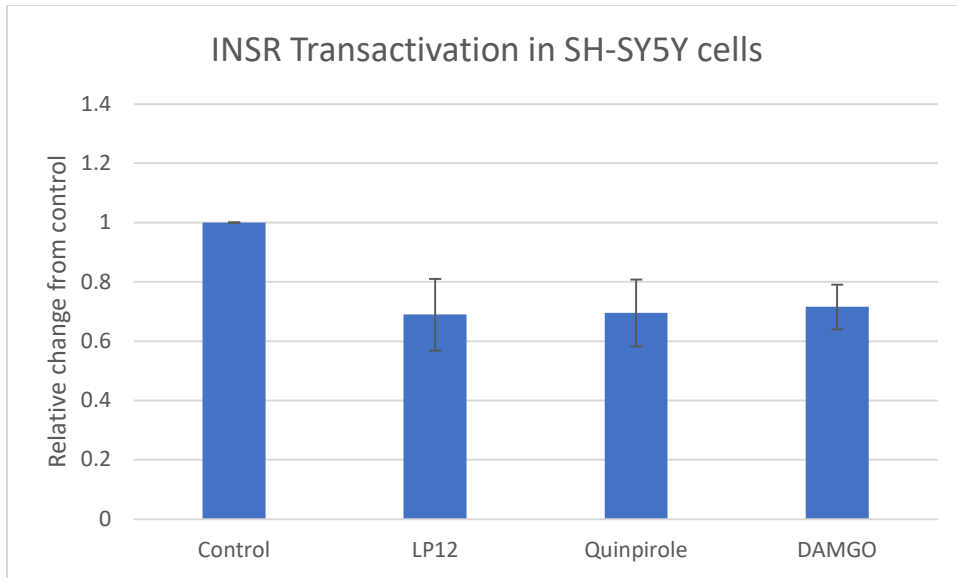


Figure 11. Effect of LP12, quinpirole, and DAMGO on insulin receptor in SH-SY5Y cells. INSR phosphorylation data was expressed as relative change compared to control. Results are shown as mean \pm SEM. Statistical analysis was done using a one-way ANOVA with Dunnett's post-hoc test ($\alpha=0.05$, $n=3$). Array images have been spliced to show appropriate dots for each RTK.

4.3 Transactivation in undifferentiated and differentiated HT22 cells

As many GPCRs are neurotransmitter receptors, an experiment was performed comparing undifferentiated and differentiated HT22 cells, to determine if the functional stage of the cell affects transactivation pathways. The results of these experiments can be seen in Figures 12 and 13. Note that these experiments were only performed once, so there were no replicates, and results may be less reliable.

The most noticeable difference between the two cell types was that in undifferentiated cells, EphA8 was expressed, and IGF-IR was not (or at least not at a level that the kit could detect), while the opposite was true in differentiated cells.

In undifferentiated cells, LP12 resulted in decreased phosphorylation for all four RTKs observed, with EphA8 showing an especially large decrease. In differentiated cells, ErbB2 was instead activated. PDGFR α was slightly higher compared to undifferentiated cells, but not meaningfully different from control. Axl and IGF-IR both showed a moderate decrease in phosphorylation.

Quinpirole instead had a slight activation effect on ErbB2 and PDGFR α in undifferentiated cells, while Axl and EphA8 showed little to no change from control. In differentiated cells, PDGFR α had a very slight increase in phosphorylation, while ErbB2, Axl, and IGF-IR remained unchanged compared to control.

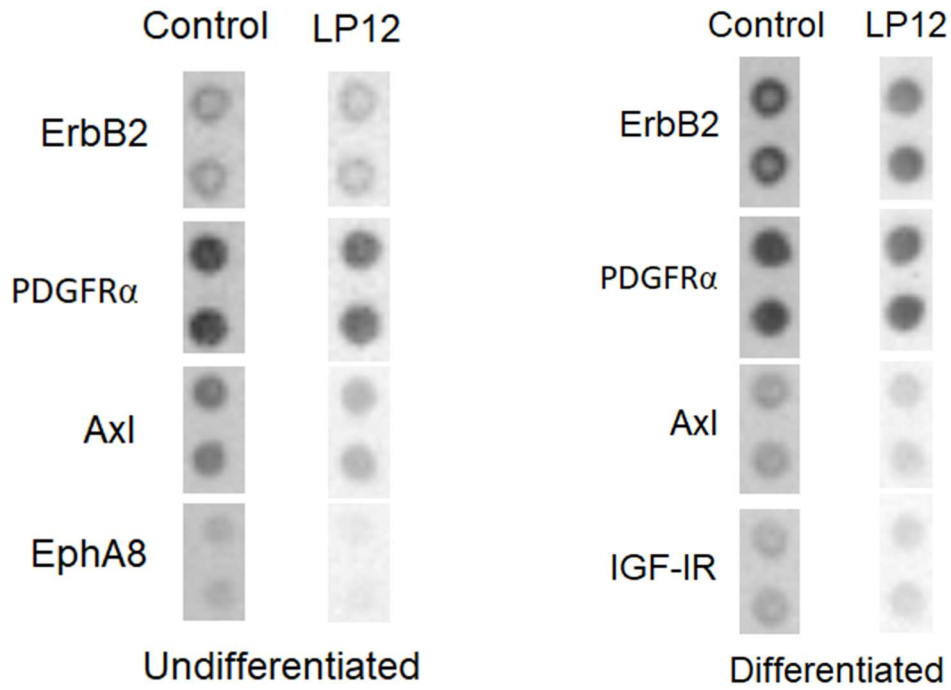
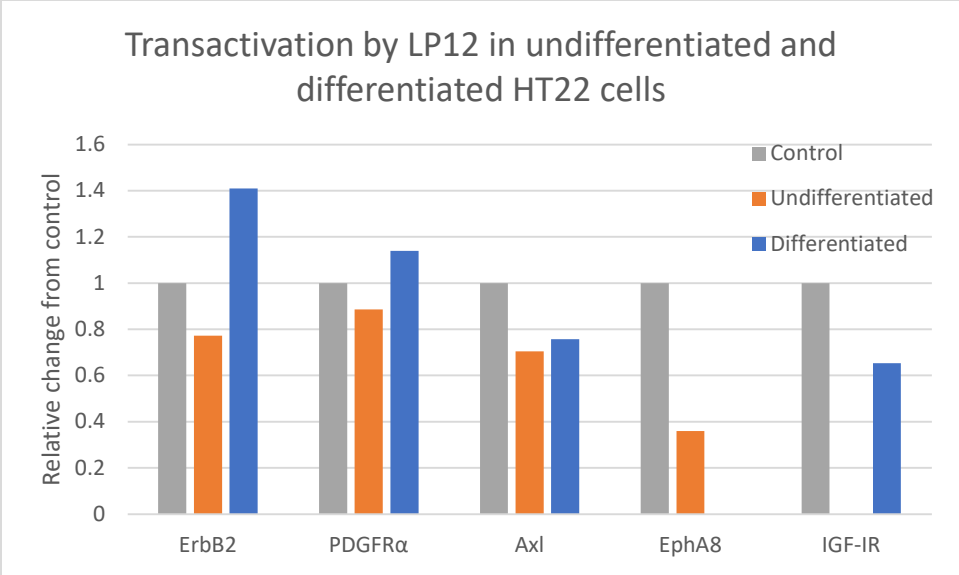


Figure 12. Effect of LP12 on ErbB2, PDGFR α , Axl, EphA8, and IGF-IR in undifferentiated and differentiated HT22 cells. RTK phosphorylation data was expressed as relative change compared to control. No statistical analysis was done as this experiment was done with a single replicate (n=1). Array images have been spliced to show appropriate dots for each RTK.

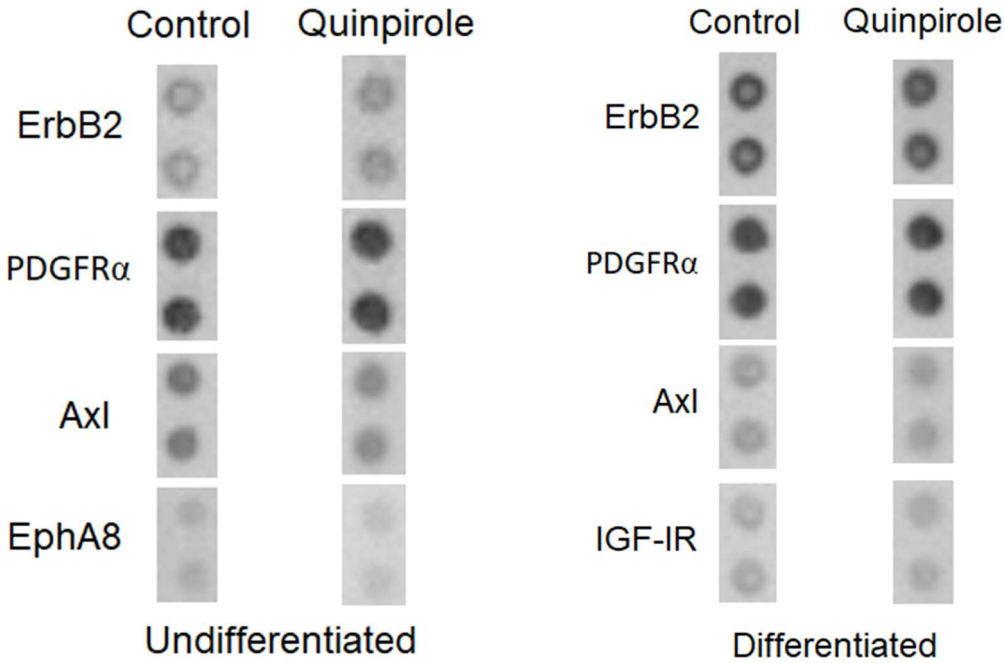
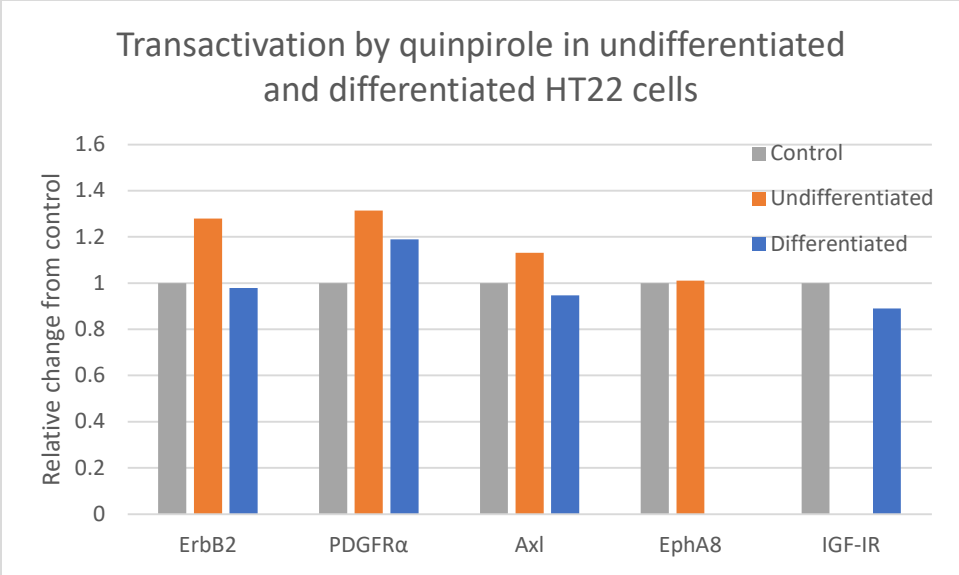


Figure 13. Effect of quinpirole on ErbB2, PDGFR α , Axl, EphA8, and IGF-IR in undifferentiated and differentiated HT22 cells. RTK phosphorylation data was expressed as relative change compared to control. No statistical analysis was done as this experiment was done with a single replicate (n=1). Array images have been spliced to show appropriate dots for each RTK.

5.0 Discussion

5.1 Transactivation of PDGFR α

Both HT22 and SH-SY5Y cells were treated with eight different GPCR agonists to determine the effect on PDGFR α and ERK phosphorylation. As ERK is a downstream target of most RTKs, its signal is indicative of transactivation from multiple RTKs as opposed to just one [1]. Results from Figures 6-9 have been summarized below in Table 9. Most results were not statistically significant, so definitive conclusions cannot be drawn. However, there are still some trends that can be discussed.

Table 9. Summary of results for transactivation of PDGFR α and activation of ERK. Increases in phosphorylation are indicated by a + sign, and decreases are indicated by a – sign. A 0 indicates there was little to no change. Statistical significance is indicated with an asterisk.

Treatment	HT22 cells, PDGFR α	HT22 cells, ERK	SH-SY5Y cells, PDGFR α	SH-SY5Y cells, ERK
LP12, 10 min	0	0	---	0
LP12, 20 min	+	–	0	–
LP44	++	–	--	0
8-OH-DPAT	+	–	--	0
Quinpirole	+++	0	–	0
CHPG	+++	0	0	+
AMN082	+++	0	0	+
DAMGO	++	–	--	+++ *
Baclofen, 1 min	+	–	0	0
Baclofen, 5 min	++	–	+	+

The serotonin receptor agonists LP12, LP44, and 8-OH-DPAT all had similar effects on both PDGFR α and ERK in both HT22 cells and SH-SY5Y cells. For all three compounds, PDGFR α signal increased in HT22 cells, but slightly decreased in SH-SY5Y cells. ERK signal decreased slightly for all three compounds, in both HT22 cells and SH-SY5Y cells. The

commonality between signalling of the three compounds may suggest that serotonin receptors share machinery involved in transactivation. Previous studies performed show that both 5-HT₇R and 5-HT_{1A}R activation result in transactivation of PDGFR β , which helps support this hypothesis [38][31]. Additionally, the reduction of ERK signal is interesting. As a downstream target of RTK signalling, it follows that its signal would decrease in response to the decrease in PDGFR α signal seen in SH-SY5Y cells. The decrease in ERK signal following serotonin receptor activation seen in HT22 cells is unusual, but is a trend seen in several other studies [39][40], indicating that this is a valid result. This result could suggest that while PDGFR α is being transactivated, other RTKs are being deactivated, causing a net decrease in ERK phosphorylation. This finding seems to be tissue-specific, as different results can be seen in HT22 cells and SH-SY5Y cells. Other studies seem to agree with this hypothesis. Studies performed show an increase in ERK phosphorylation in hypothalamic paraventricular nucleus and dorsal raphe nucleus of the brainstem in adult rats following systemic 5-HT_{1A}R activation *in vivo* [41][42]. In rat cortex, no change in ERK was seen, while in rat hippocampus, a decrease was seen following activation of 5-HT_{1A}R [40][41]. As HT22 cells are hippocampal-derived, this is especially interesting. The fact that both mouse and rat hippocampal cells respond similarly suggests that, while transactivation is a tissue-specific process, these pathways may be conserved between species.

Quinpirole, the D₂R agonist, had a strong activation effect on PDGFR α in HT22 cells, but a slight reduction in SH-SY5Y cells. ERK signal was reduced in both cell types. These results seem to suggest that transactivation of PDGFR α by quinpirole is occurring in HT22 cells, but not SH-SY5Y cells. It is possible that this transactivation pathway is occurring in a cell-type-dependent manner. The reduction in ERK signal would seem to suggest that deactivation of

RTKs, and therefore the MAPK/ERK pathway, is occurring. There is, however, reason to question the validity of this result. A time course experiment performed prior showed a large increase in ERK activity at the time point used, which disagrees with the findings of this experiment. The data for this can be seen in the Appendix, Figure 20. Additionally, other studies have shown increases in ERK phosphorylation following activation of D2R ^[43], as well as other dopamine receptors ^[44]. It would be worthwhile to investigate this further with more replicates, to verify which result is correct.

The metabotropic glutamate receptor agonists CHPG and AMN082 both had similar effects. There was a large activation effect on PDGFR α in HT22 cells, but signal remained relatively unchanged in SH-SY5Y cells. There was little to no effect on ERK in HT22 cells, but in SH-SY5Y, there was a slight increase in signal from both treatments. These results are very similar to each other, which may suggest that they share the machinery involved in transactivation. The slight difference in effect seen on ERK in HT22 cells in Figure 7 could easily be due to variance, which would make the results for the two compounds almost identical. In HT22 cells, the large increase in PDGFR α signal combined with the lack of change in ERK suggests that while PDGFR α is being transactivated, other pathways are deactivating ERK. In SH-SY5Y cells, it instead seems that, while ERK is being activated, it is not through PDGFR α . This would indicate that there are multiple separate transactivation pathways that CHPG and AMN082 can initiate that are dependent on cell-type. One study showed that, in astrocytes, ERK activation is reliant on EGFR ^[33], which provides a possible alternative pathway.

DAMGO, the MOR agonist, had a moderate activation effect on PDGFR α in HT22 cells, but a slight reduction in ERK signal. In SH-SY5Y cells, it caused a decrease in PDGFR α but a large increase in ERK signal. As with other agonists, this seems to indicate the pathway is active

in HT22 cells but not in SH-SY5Y cells. The large increase in ERK signal seen in SH-SY5Y cells indicates there are likely other active transactivation pathways. Several transactivation pathways involving MOR have been observed in other studies, including transactivation of EGFR ^{[45][34]} and VEGFR ^[46]. Furthermore, MOR-induced ERK activation has been well-studied in several cell types, with studies identifying several key components of the pathway, including phosphokinase C, G-protein-coupled receptor kinase 3, and arrestin ^[47].

Baclofen, the GABA β R agonist activated PDGFR α in both HT22 and SH-SY5Y cells, with the effect being more pronounced in HT22 cells. For ERK, there was a decrease in signal in HT22 cells, but an increase in signal in SH-SY5Y cells. Interestingly, this is the only result for which PDGFR α was activated in SH-SY5Y cells, suggesting that in this case, the same pathway may be active in both cell types. However, due to the magnitude of the signal being considerably larger in HT22 cells, it may be that certain factors are present or absent in one cell type or the other. Studies have observed several proteins that are required for transactivation pathways involving GABA β R. In primary cerebellar granule neuronal cultures, Gi/o-protein, PLC, cytosolic Ca²⁺, and FAK1 were shown to be required for transactivation of IGF-1 receptor to occur ^[48]. The deactivation of ERK seen in HT22 cells is inconsistent with other studies. Multiple other sources have shown an increase in ERK phosphorylation following treatment with baclofen ^{[35][49]}, even when also using HT22 cells ^[35]. Because of this, it is possible that the reduction in ERK signal seen in HT22 cells is an erroneous result. Additional replicates of this experiment could help reveal which is correct.

In summary, all compounds used resulted in PDGFR α transactivation in HT22 cells while ERK signal either decreased or remained unchanged. This commonality across all compounds tested is interesting. It could suggest that, in this cell type, transactivation occurs non-

specifically, where any GPCR activity will result in PDGFR α transactivation. The reduction in ERK signal seen in almost all cases would corroborate the idea that transactivation is occurring non-specifically. Further research into the mechanisms behind PDGFR α transactivation could help elucidate this point. In SH-SY5Y cells, PDGFR α signal decreased for all treatments except baclofen, which caused an increase. ERK signal changes were dependent on treatment used, with CHPG, AMN082, DAMGO, and baclofen resulting in increased signal, and LP12, LP44, 8-OH-DPAT, and quinpirole resulting in decreased or unchanged signal. Overall, in this cell type, transactivation seems to be much more dependent on the compound used, which suggests that transactivation is acting in specific GPCR-RTK pairs. Taken together, these results provide strong evidence that transactivation is a highly tissue-specific process, with different cell types expressing very different transactivation pathways.

5.2 Transactivation by LP12, Quinpirole, and DAMGO

To observe the transactivation effects of a given GPCR on a wide variety of RTKs at once, the Proteome Profiler Phospho-RTK Array kit was used with both HT22 and SH-SY5Y cells.

HT22 cells were treated with quinpirole, activating D2R. As seen in Figure 10, for all 4 RTKs observed (ErbB2, PDGFR α , Axl, IGF-IR), there was little to no change in signal. The lack of change would seem to suggest that no transactivation occurred following treatment with quinpirole. However, western blot analysis in section 3.1, Figure 6 showed a large increase in PDGFR α activation following quinpirole treatment. Since the phospho-RTK kit uses anti-phospho-tyrosine antibody for detection, it is possible that, while tyrosine residue 849 was

transactivated by quinpirole, other residues were deactivated, resulting in no overall change in phosphorylation. This presents the possibility that, in the case of this transactivation pathway, a specific residue is being targeted. Since ligand-dependent transactivation pathways make use of an RTK's native ligand, this would indicate the pathway is ligand-independent. It is worth noting that there exist both ligand-independent and ligand-dependent pathways involving dopamine receptors. In one study, transactivation of EGFR by D2R occurred via a ligand-dependent mechanism using ADAM10 and ADAM17 [32]. Conversely, another study showed that transactivation of PDGFR β by D4R did not require ADAMs or dimerization of PDGFR β indicating it was a ligand-independent mechanism [50]. IGF-1R phosphorylation changed minimally, which would either suggest that no transactivation or deactivation occurred, or that both occurred, resulting in some tyrosine residues becoming more phosphorylated, and others becoming less phosphorylated, resulting in no visible change. Another study showed that D2R activation can inhibit IGF-1R phosphorylation in AGS cells [51]. These cells are epithelial cells isolated from stomach tissue, so the pathway may not be expressed the same way in the neuronal HT22 cells, but it is a possibility that IGF-1R is inhibited through this pathway, and activated through another in HT22 cells, resulting in what was seen.

Unfortunately, there does not seem to be research on transactivation of ErbB2 or Axl by dopamine receptors, so all that can be said about those results is that it appears no transactivation occurred. There is research on transactivation of ErbB2 by other GPCRs, however. Of particular note is transactivation by PAR1. As previously mentioned, PARs are implicated in certain cancers, with breast cancer being most prominent [52]. ErbB2 is commonly overexpressed in breast cancers [53], making transactivation by PAR1 an excellent candidate for cancer research involving transactivation pathways.

SH-SY5Y cells were treated with LP12, quinpirole, or DAMGO. Unfortunately, the only RTK that was able to be detected by the kit was INSR. All three treatments resulted in decreased phosphorylation of INSR. This suggests that transactivation of INSR by LP12, quinpirole, and DAMGO is not occurring, but in fact they are causing a decrease in INSR phosphorylation. Though direct transactivation or deactivation of INSR by serotonin, dopamine, and opioid receptors has not been observed in other studies, there are some possible explanations to the effect seen. One study observes crosstalk between serotonin receptors and INSR, showing that both receptors activate phosphoinositide 3-kinase and Akt ^[54]. Pre-treatment with insulin blocked the ability of serotonin to activate Akt, demonstrating feedback mechanisms that affect both receptors ^[54]. Another study shows similar results with MOR. DAMGO treatment and insulin treatment were shown to both activate the MAPK/ERK pathway. However, treatment with DAMGO also resulted in desensitization to insulin treatment ^[55], again demonstrating a similar feedback system to that seen with serotonin. Whether these findings were transactivation or a different pathway that similarly affects ERK is unclear. However, they show a feedback mechanism that could be resulting in what is seen in this experiment's reduced INSR signal.

Overall, the results of this experiment were somewhat disappointing. The phospho-RTK kits used contained antibodies to 39 and 49 RTKs for the mouse and human kits, respectively. However, only 4 RTKs in HT22 cells and 1 RTK in SH-SY5Y cells produced enough signal to be detected by the kit. Because of this, the intended analysis determining which RTKs can be transactivated by a given GPCR agonist was unsuccessful. There are a number of potential solutions to this problem going forward. One would be to use a different cell line; preferably one known to express many fully functional RTKs. Finding a cell line that natively expresses all these genes for many RTKs simultaneously would be difficult, requiring a thorough search of

literature, and likely a significant amount of trial and error. Transforming a cell line with several constitutively expressed RTK genes could also be possible, but it would likely lack the necessary supporting proteins necessary for transactivation to occur, such as the appropriate MMP proteins, or the pro-ligand to be cleaved from the surface of the cell. Another solution is to instead alter the protocol. There are other phospho-RTK kits available, and using a different one could produce different, hopefully better results. The Human RTK Phosphorylation Array C1 (RayBio AAH-PRTK-1-2) and the Human RTK Phosphorylation Antibody Array (abcam ab193662) are two possibilities that each contain antibodies to 71 different targets including both RTKs and some PTKs. The larger number of assessed RTKs may improve the chances that some will be able to be observed. Alternatively, instead of using kits, standard western blotting using phospho-RTK antibodies would work. Since antibody to a single phospho-tyrosine is used, it is inherently a more sensitive method and can be normalized to a loading control to further improve sensitivity. However, this method would require limiting the number of RTKs observed, as it would be extremely labour-intensive to perform 39-71 separate western blots to match the number of RTKs assessed by one of the kits.

The large number of RTKs unobserved in SH-SY5Y cells is quite unexpected and worth mentioning. As SH-SY5Y cells are a cancer cell line, RTKs would be expected to be expressed at higher levels than normal, but this does not seem to be the case. Indeed, many RTKs have been observed in SH-SY5Y cells, including ROR1, ROR2, and PDGFR α [56], which was also seen in experiments within this thesis. This could indicate that the Proteome Profiler kit is not sensitive enough to detect these RTKs, making it unsuitable for these experiments.

5.3 Transactivation in undifferentiated and differentiated HT22 cells

Undifferentiated and differentiated HT22 cells were tested to determine if the stage of cell development influences transactivation. This experiment was not performed in replicate, so results may not be reliable.

Transactivation by LP12 caused a decrease in phosphorylation of ErbB2 and PDGFR α in undifferentiated HT22 cells, but an increase in phosphorylation in differentiated cells. This could indicate that these transactivation pathways are not expressed until cells are differentiated. Phosphorylation of Axl is relatively unchanged between undifferentiated and differentiated cells, with both showing a decreased signal. EphA8 is only seen in undifferentiated cells and has a large decrease in phosphorylation. In differentiated cells, IGF-1R is seen instead, and also has a large decrease in phosphorylation. As there is very little research on undifferentiated cells, it is difficult to determine if the results seen are valid.

Transactivation by quinpirole was higher for ErbB2, PDGFR α , and Axl in undifferentiated cells compared to differentiated cells. In differentiated cells, there is very little change compared to the control. This could suggest that these transactivation pathways are lost after differentiation, or that other pathways are gained that deactivate the RTK targets in addition to the transactivation seen. Another possibility is that the differentiated cells are experiencing excitotoxic effects. Multiple studies have shown that differentiated HT22 cells are more susceptible to excitotoxicity ^{[57][58]}, which could explain the reduction in signal. EphA8 is seen in undifferentiated cells with no change compared to the control, indicating it likely has no transactivation activity in these cells. In differentiated cells, IGF-1R is seen with a small decrease in phosphorylation.

The loss of EphA8 upon differentiation may be explained by the role ephrin receptors play in cell development. They function in axon guidance during embryonic development by binding to ephrins on opposing cells, tethering them together ^[59]. As this is a developmental process, it follows that ephrins and their receptors would be downregulated upon differentiation.

IGF-IR's presence in differentiated but not undifferentiated cells may be explained by the differentiation protocol used. The N2 supplement used contains insulin, which may be stimulating the cells to upregulate expression of IGF-IR. This would also explain why INSR was seen in differentiated SH-SY5Y cells in Figure 11.

6.0 Conclusions and future directions

The primary purpose of this thesis was to capture the scope of transactivation; Determining which GPCRs are capable of transactivation, which RTKs can be transactivated, whether GPCR and RTK families share similarities in transactivation pathways, and whether transactivation is dependent on cell type.

Some aspects of this were successful. Despite most results not being statistically significant, there were some meaningful trends observed. The results suggest that GPCR receptor families may share some transactivation machinery, and that cell type has a significant effect on transactivation. There seems to be strong evidence that transactivation is not the only pathway in effect upon GPCR activation, as proteins downstream of activated RTKs are instead being deactivated. On the other hand, some aspects were not successful. The phospho-RTK kit produced far fewer results than expected, making it impossible to draw any conclusions in regard to which RTKs are able to be transactivated.

Due to the broad nature of this thesis, and the lack of success in certain areas, there is a wide array of possible avenues for future research. Addressing the unsuccessful experiments is one such avenue, as the intention behind the experiments is still important. Attempting the experiment using different cell lines or other phospho-RTK array kits would be a good starting point to solve the problem, and completing this experiment would provide important insight into the scope of transactivation, making it worthwhile. Another avenue would be to attempt to look at certain trends in more detail. The results showed that GPCR receptor families may share transactivation machinery, but this experiment was too broad to determine that with any certainty. Attempting to look more closely at the downstream targets of 5-HT_{1A}R, 5-HT₇R, and other serotonin receptors, or mGluR₅, mGluR₇, and other metabotropic glutamate receptors

could provide valuable insight into whether or not GPCR receptor families follow the same mechanisms of transactivation. A third possible avenue of research would be to look more closely at ERK. Several of the results involving ERK seemed to go against expectations, and diving deeper into the mechanisms involving ERK signaling downstream of both GPCRs and RTKs would be valuable in understanding the mechanisms of cellular signaling. Finally, there were many GPCR-RTK pairs that were observed only briefly. Studying them in greater detail is an important step in furthering our understanding of transactivation.

References

- [1] Alberts B. et al. (2015). *Molecular biology of the cell* (6th edition). New York, NY: Garland Science. pp. 813-888.
- [2] Katrich V. et al. (2012). Diversity and Modularity of G-Protein Coupled Receptor Structures. *Trends Pharmacol Sci.* 33(1): 17-27.
- [3] Hu G., Mai T., & Chen C. (2017). Visualizing the GPCR Network: Classification and Evolution. *Scientific Reports* 7: 15495
- [4] Gurevich V. & Gurevich E. (2019). GPCR Signalling Regulation: The Role of GRKs and Arrestins. *Front Pharmacol.* 10: 125.
- [5] Velazhahan V. et al. (2020). Structure of the Class D GPCR Ste2 dimer coupled to two G proteins. *Nature* 589: 148-153
- [6] Mato J. M. & Konijn T. M. (1975). Chemotaxis and Binding of Cyclic AMP in Cellular Slime Molds. *Biochimica et Biophysica Acta* 385: 173-179.
- [7] Schulte G. & Koziellewicz P. (2019). Structural insights into Class F receptors – What have we learnt regarding agonist-induced activation? *Basic Clin Pharmacol Toxicol* 126(Suppl. 6): 17-24
- [8] Sriram K. & Insel P. A. (2017). G Protein-Coupled Receptors as Targets for Approved Drugs: How Many Targets and How Many Drugs? *Mol Pharmacol* 93: 251-258.
- [9] Hauser A. S. et al. (2017). Trends in GPCR drug discovery: new agents, targets, and indications. *Nature Reviews Drug Discovery* 16: 829-842.

- [10] Lemmon M. & Schlessinger J. (2010). Cell Signalling by receptor-tyrosine kinases. *Cell* 141(7): 1117-1134.
- [11] Segaliny et al. (2012). Receptor tyrosine kinases: Characterisation, mechanism of action and therapeutic interests for bone cancer. *Journal of Bone Oncology* 4: 1-12.
- [12] Wang K. et al. (2019). Apoptosis of cancer cells is triggered by selective crosslinking and inhibition of receptor tyrosine kinases. *Communications Biology* 2: 231
- [13] Du Z. & Lovly C. M. (2018). Mechanisms of receptor tyrosine kinase activation in cancer. *Molecular Cancer* 17: 58
- [14] Pearson G. et al. (2001). Mitogen-Activated Protein (MAP) Kinase Pathways: Regulation and Physiological Functions. *Endocrine Reviews* 22(2): 153-183.
- [15] Guo Y. et al. (2019). ERK/MAPK signalling pathway and tumorigenesis (Review). *Experimental and Therapeutic Medicine* 19: 1997-2007
- [16] Yamaoka T et al. (2018). Receptor Tyrosine Kinase-Targeted Cancer Therapy. *Int. J. Mol. Sci.* 19: 3491.
- [17] Metibemu D. S. et al. (2019). Exploring receptor tyrosine kinases- inhibitors in Cancer treatments. *Egyptian Journal of Medical Human Genetics* 20: 35.
- [18] Hojjat-Farsangi M. (2014). Small-Molecule Inhibitors of the Receptor Tyrosine Kinases: Promising Tools for Targeted Cancer Therapies. *Int. J. Mol. Sci.* 15: 13768-13801.
- [19] Daub H. et al. (1996). Role of transactivation of the EGF receptor in signalling by G-protein-coupled receptors. *Nature* 379, 8, 557-560

- [20] Cattaneo F. et al. (2014). Cell-Surface Receptors Transactivation Mediated by G-Protein Coupled Receptors. *Int. J. Mol. Sci.* 15, 19700-19728.
- [21] Kilpatrick L. E. & Hill S. J. (2021). Transactivation of G protein-coupled receptors (GPCRs) and receptor tyrosine kinases (RTKs): Recent insights using luminescence and fluorescence technologies. *Curr Opin Endocr Metab Res.* 16: 102-112.
- [22] Roelle S. et al. (2003). Matrix metalloproteinase 2 and 9 mediate epidermal growth factor receptor transactivation by gonadotropin-releasing hormone. *J Biol Chem.* 278(47): 47307-47318.
- [23] Shah B. H. et al. (2003). Roles of Src and Epidermal Growth Factor Receptor Transactivation in Transient and Sustained ERK1/2 Responses to Gonadotropin-releasing Hormone Receptor Activation. *J Biol Chem.* 278(21): 19118-19126.
- [24] Liberto V. D., Mudo G., & Belluardo N. (2018). Crosstalk between receptor tyrosine kinases (RTKs) and G protein-coupled receptors (GPCRs) in the brain: Focus on heteroreceptor complexes and related functional neurotrophic effects. *Neuropharmacology* 152: 67-77.
- [25] Kruk J. S. et al. (2013). Reactive Oxygen Species Are Required for 5-HT-Induced Transactivation of Neuronal Platelet-Derived Growth Factor and TrkB Receptors, but not for ERK1/2 Activation. *PLoS ONE* 8(9): e77027.
- [26] Vasefi M. & Beazely M. A. (2020). Neuroprotective effects of direct activation and transactivation of PDGF β receptors. *Vessel Plus* 4: 24

- [27] Dorsam R. T. & Gutkind J. S. (2007). G-protein-coupled receptors and cancer. *Nature Reviews Cancer* 7: 79-94
- [28] Arakaki A. K. S. et al. (2018). GPCRs in Cancer: Protease-Activated Receptors, Endocytic Adaptors and Signaling. *Int. J. Mol. Sci.* 19: 1886.
- [29] Usman S. et al. (2020). The current status of anti-GPCR drugs against different cancers. *Journal of Pharmaceutical Analysis* 10: 517-521.
- [30] Samarajeewa A. et al. (2014). 5-HT₇ receptor activation promotes an increase in TrkB receptor expression and phosphorylation. *Front Behav Neurosci* 8: 391
- [31] Kruk et al. (2013). 5-HT_{1A} receptors transactivate the platelet-derived growth factor receptor type beta in neuronal cells. *Cellular Signaling* 25: 133-143
- [32] Yoon S. & Baik J. (2013). Dopamine D₂ Receptor-mediated Epidermal Growth Factor Receptor Transactivation through a Disintegrin and Metalloprotease Regulates Dopaminergic Neuron Development via Extracellular Signal-related Kinase Activation. *The Journal of Biological Chemistry* 288 (40): 28435-28446
- [33] Peavy R. D. et al. (2001). Metabotropic Glutamate Receptor 5-Induced Phosphorylation of Extracellular Signal-Regulated Kinase in Astrocytes Depends on Transactivation of the Epidermal Growth Factor Receptor. *The Journal of Neuroscience* 21 (24): 9619-9628
- [34] Belcheva M. M. et al. (2003). μ Opioid Transactivation and Down-Regulation of the Epidermal Growth Factor Receptor in Astrocytes: Implications for Mitogen-Activated Protein Kinase Signaling. *Molecular Pharmacology* 64(6): 1391-1401.

- [35] Im B. & Rhim H. (2012). GABAB receptor-mediated ERK1/2 phosphorylation via a direct interaction with Cav1.3 channels. *Neuroscience Letters* 513: 89-94
- [36] He M. et al. (2013). Differentiation renders susceptibility to excitotoxicity in HT22 neurons. *Neural Regen Res.* 8(14): 1297-1306.
- [37] Feles S. et al. (2022). Streamlining Culture Conditions for the Neuroblastoma Cell Line SH-SY5Y: A Prerequisite for Functional Studies. *Methods Protoc* 5(4): 58
- [38] Vasefi M. S. et al. (2012). Activation of 5-HT7 receptors increases neuronal platelet-derived growth factor B expression. *Neuroscience Letters* 511: 65-69
- [39] Wang Q. et al. (2014). 5-HT1A receptor-mediated phosphorylation of extracellular signal-regulated kinases (ERK1/2) is modulated by regulator of G protein signaling protein 19. *Cellular Signaling* 26(9): 1846-1852
- [40] Chen J. et al. (2002). 5-HT1A receptor-mediated regulation of mitogen-activated protein kinase phosphorylation in rat brain. *European Journal of Pharmacology* 452: 155-162
- [41] Masson J. et al. (2012). Serotonergic signaling: multiple effectors and pleiotropic effects. *WIREs Membr Transp Signal* 1:685-713, doi: 10.1002/wmts.50
- [42] Sullivan N. R. et al. (2005). Tansospirone activates neuroendocrine and ERK (MAP kinase) signaling pathways specifically through 5-HT1A receptor mechanisms in vivo. *Naunyn-Schmiedeberg's Arch Pharmacol* 371: 18-26
- [43] Wang C. et al. (2005). Dopamine D2 receptor stimulation of mitogen-activated protein kinase mediated by cell type-dependent transactivation of receptor tyrosine kinases. *Journal of Neurochemistry* 93: 899-909

- [44] Kruk J. et al. (2014). Transactivation of Receptor Tyrosine Kinases by Dopamine Receptors. *Neuromethods* 96: 211-227
- [45] Araldi D. et al. (2018). Role of GPCR (Mu-Opioid)-RTK (Epidermal Growth Factor) Crosstalk in Opioid-Induced Hyperalgesic Priming (Type II). *Pain* 159 (5): 864-875
- [46] Stephenson E. J. (2005). μ Opioid Receptor Stimulates a Growth Promoting and Pro-Angiogenic Tumor Microenvironment by Transactivating VEGF Receptor-2/Flk-1. *Blood* 106(11): 3687.
- [47] Al-Hasani R. & Bruchas M. R. (2011). Molecular Mechanisms of Opioid Receptor-Dependent Signaling and Behavior. *Anesthesiology* 115 (6): 1363-1381
- [48] Tu H. et al. (2010). GABAB Receptor Activation Protects Neurons from Apoptosis via IGF-1 Receptor Transactivation. *The Journal of Neuroscience* 30 (2): 749-759
- [49] Xia S. et al. (2017). GABABR-Induced EGFR Transactivation Promotes Migration of Human Prostate Cancer Cells. *Mol Pharmacol* 92: 265-277
- [50] Chi S. S. et al. (2010). Transactivation of PDGFRb by dopamine D4 receptor does not require PDGFRb dimerization. *Molecular Brain* 3, 22
- [51] Ganguly S. et al. (2010). Dopamine, by Acting through Its D2 Receptor, Inhibits Insuline-Like Growth Factor-I (IGF-I)-Induced Gastric Cancer Cell Proliferation via Up-Regulation of Kruppel-Like Factor 4 through Down-Regulation of IGF-IR and AKT Phosphorylation. *Am J Pathol.* 177 (6): 2701-2707
- [52] Arora P. et al. (2008). Persistent transactivation of EGFR and ErbB2/HER2 by protease-activated receptor-1 promotes breast carcinoma cell invasion. *Oncogene* 27: 4434-4445.

- [53] Mitri Z., Constantine T., & O'Regan R. (2012). The HER2 Receptor in Breast Cancer: Pathophysiology, Clinical Use, and New Advances in Therapy. *Chemother Res Pract.* 2012: 743193.
- [54] Papazoglou I. et al. (2012). Hypothalamic serotonin-insulin signaling cross-talk and alterations in a type 2 diabetic model. *Molecular and Cellular Endocrinology* 350: 136-144
- [55] Li Y. et al. (2003). Morphine Induces Desensitization of Insulin Receptor Signaling. *Mol Cell Biol* 23 (17): 6255-6266
- [56] Rozen E. J. & Shohet J. M. (2022). Systemic review of the receptor tyrosine kinase superfamily in neuroblastoma pathophysiology. *Cancer and Metastasis Review* 41: 33-52.
- [57] He M. et al. (2013). Differentiation renders susceptibility to excitotoxicity in HT22 neurons. *Neural Regeneration Research* 8 (14): 1297-1306
- [58] Zhao Z. et al. (2013). Differentiation of HT22 neurons induces expression of NMDA receptors that mediates homocysteine cytotoxicity.
- [59] Egea J. & Klein R. (2007). Bidirectional Eph-ephrin signaling during axon guidance. *Trends in Cell Biology* 17(5): 230-238.

Appendix

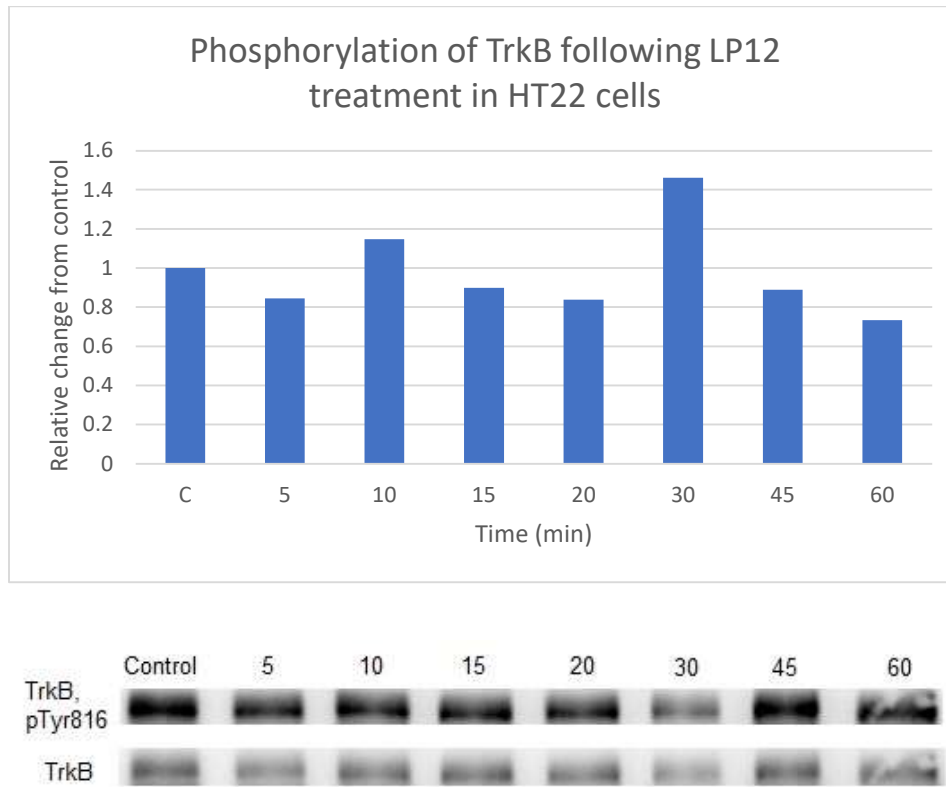


Figure 14. Time course of TrkB phosphorylation following LP12 treatment. pTrkB data were normalized to total TrkB expression and expressed as relative change compared to control. No statistical analysis was done as this experiment was done with a single replicate (n=1). Western blot images have been spliced to better align bands.

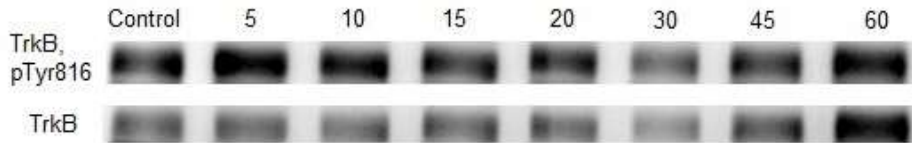
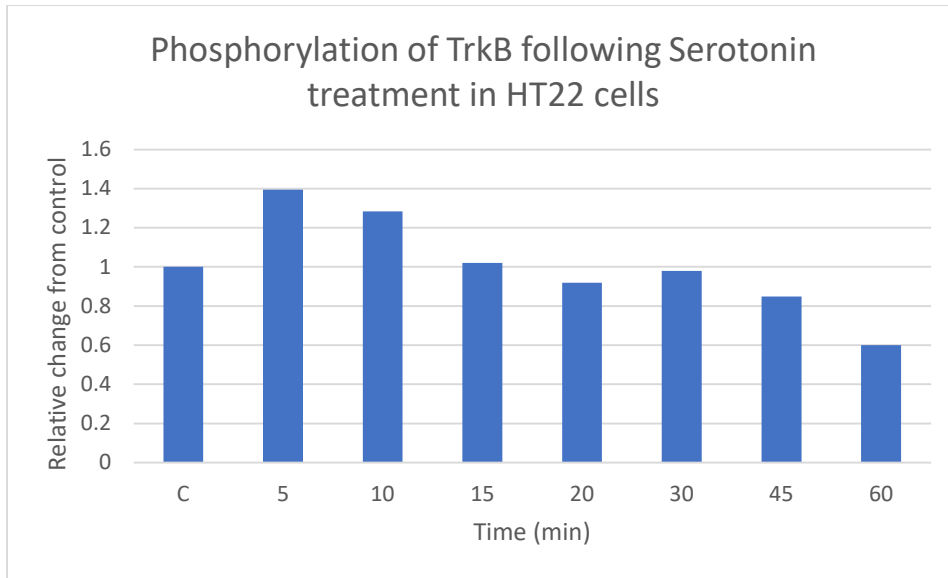


Figure 15. Time course of TrkB phosphorylation following serotonin treatment. pTrkB data were normalized to total TrkB expression and expressed as relative change compared to control. No statistical analysis was done as this experiment was done with a single replicate (n=1). Western blot images have been spliced to better align bands.

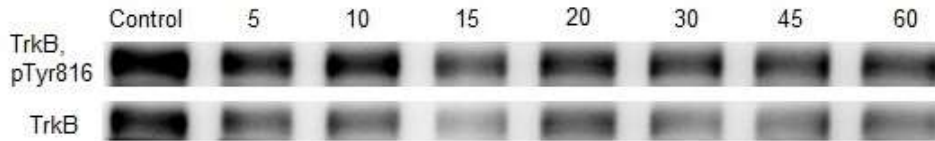
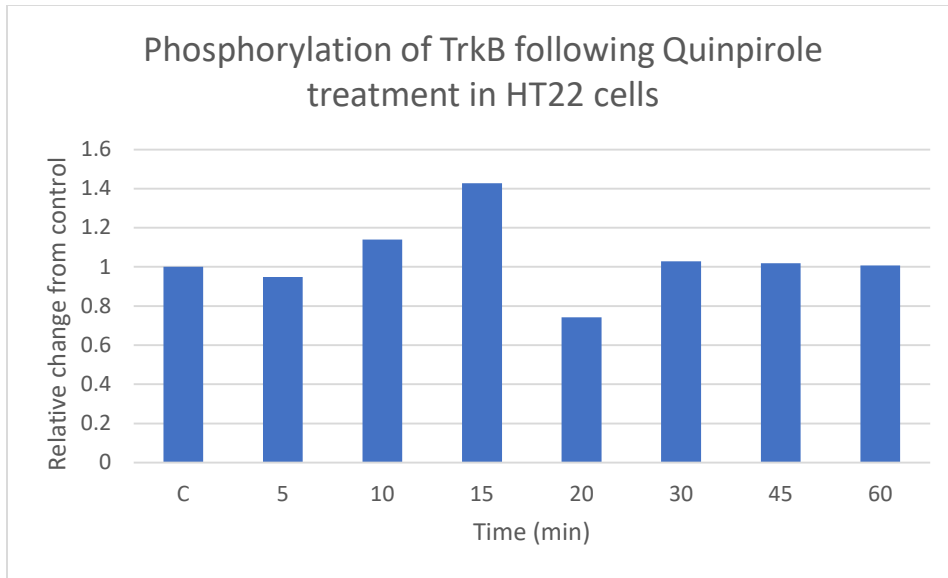


Figure 16. Time course of TrkB phosphorylation following quinpirole treatment. pTrkB data were normalized to total TrkB expression and expressed as relative change compared to control. No statistical analysis was done as this experiment was done with a single replicate (n=1). Western blot images have been spliced to better align bands.

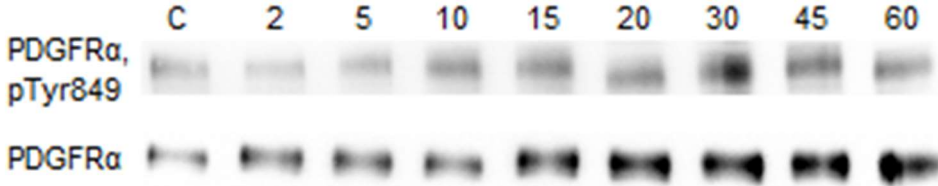
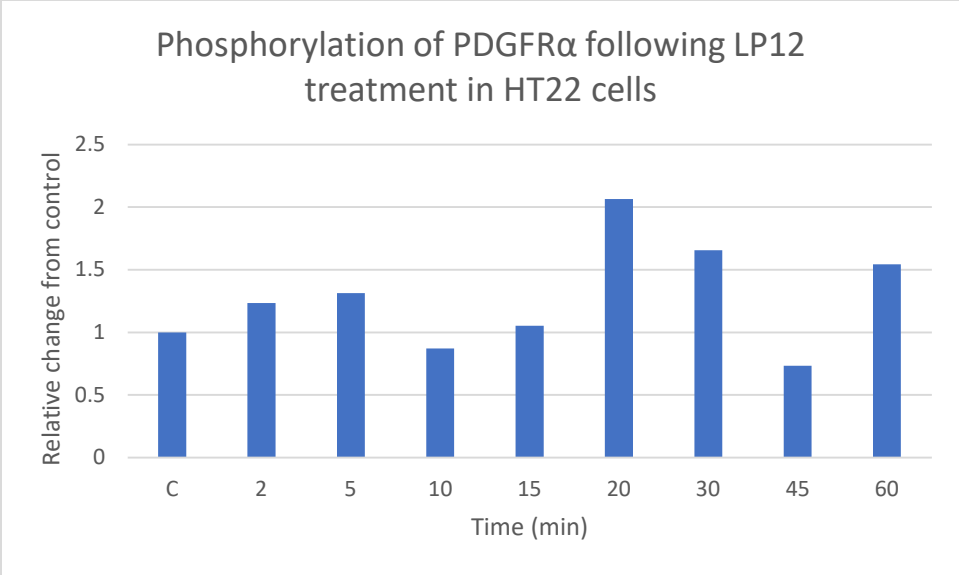


Figure 17. Time course of PDGFR α phosphorylation following LP12 treatment. pPDGFR α data were normalized to total PDGFR α expression and expressed as relative change compared to control. No statistical analysis was done as this experiment was done with a single replicate (n=1). Western blot images have been spliced to better align bands.

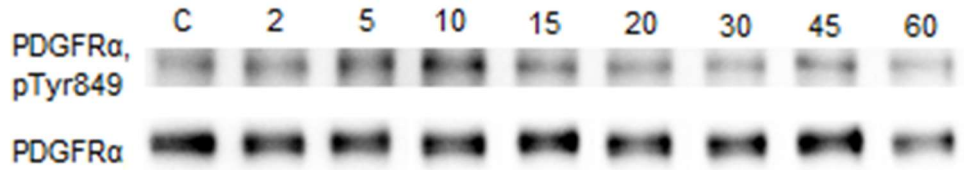
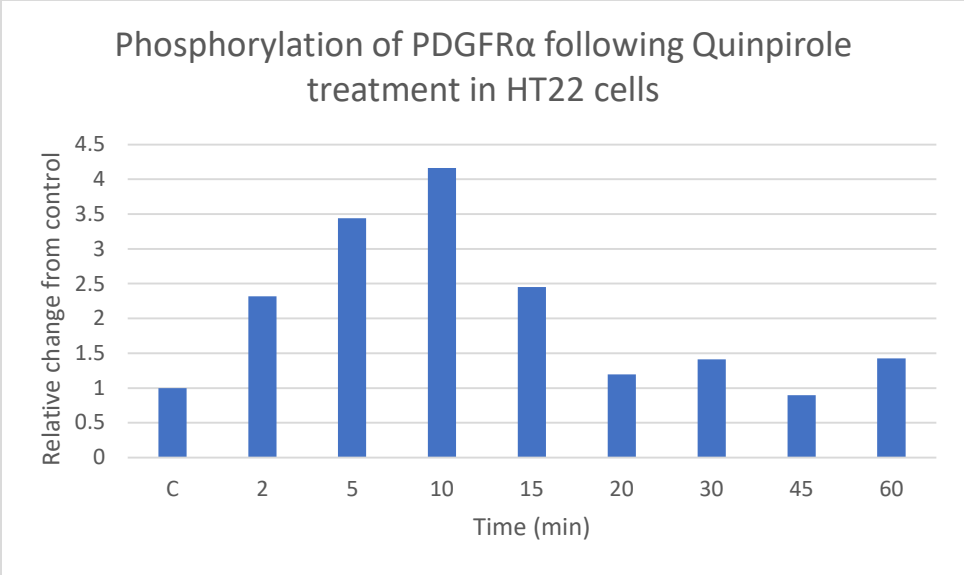


Figure 18. Time course of PDGFR α phosphorylation following quinpirole treatment. pPDGFR α data were normalized to total PDGFR α expression and expressed as relative change compared to control. No statistical analysis was done as this experiment was done with a single replicate (n=1). Western blot images have been spliced to better align bands.

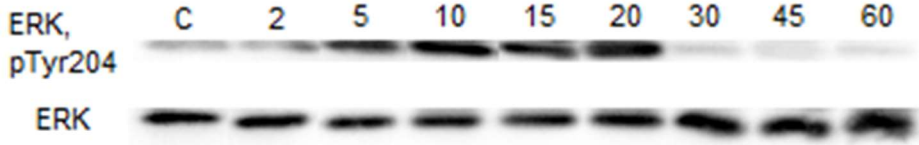
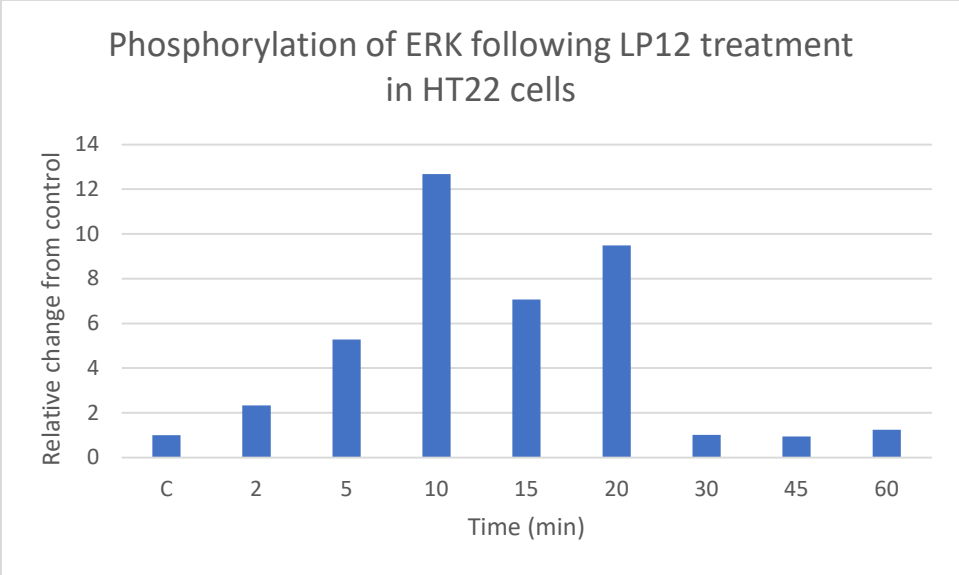


Figure 19. Time course of ERK phosphorylation following LP12 treatment. pERK data were normalized to total ERK expression and expressed as relative change compared to control. No statistical analysis was done as this experiment was done with a single replicate (n=1). Western blot images have been spliced to better align bands.

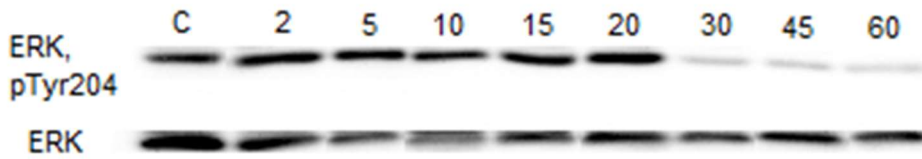
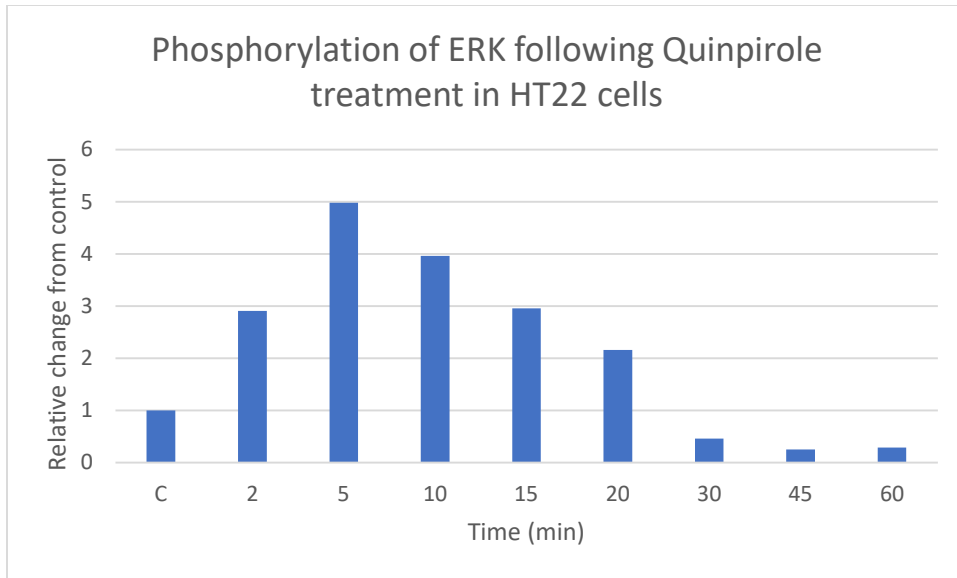


Figure 20. Time course of ERK phosphorylation following quinpirole treatment. pERK data were normalized to total ERK expression and expressed as relative change compared to control. No statistical analysis was done as this experiment was done with a single replicate (n=1). Western blot images have been spliced to better align bands.



Figure 21. Imaged array membrane showing effects of PDGF-AA treatment in HT22 cells. Sample applied to membrane M0287 was the vehicle control, while sample applied to membrane M0288 was treated with PDGF-AA. There was an 8-fold increase in PDGFR α phosphorylation, with no changes to the other RTKs, demonstrating that PDGFR α is present and functional in HT-22 cells. Note that dots in the top left, top right, and bottom right corners are for alignment, and do not represent RTKs.